Active Tremor Compensation in Handheld Instrument for Microsurgery

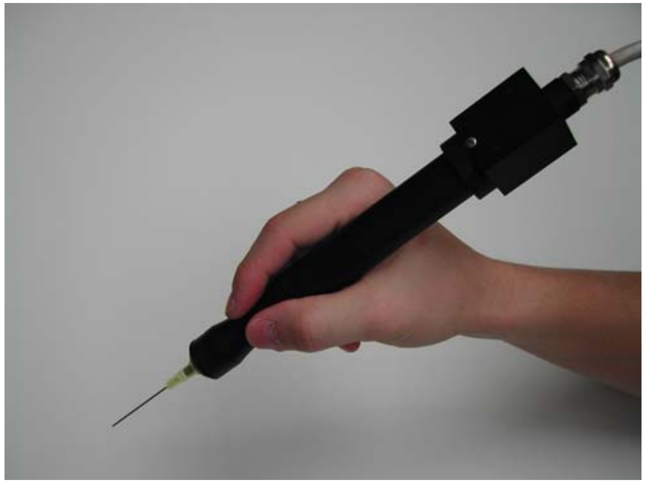

Wei Tech Ang
School of Mechanical & Aerospace Engineering
Nanyang Technological University
Singapore
wtang@ntu.edu.sg

NANYANG TECHNOLOGICAL UNIVERSITY

Contributors

- Cameron N. Riviere
  Associate Research Professor 
- David Y. Choi 
  Ph.D. Student
- Si Yi Khoo
  Research Engineer

- Wei Tech Ang 
  Assistant Professor
- Mounir Krichane 
  Exchange Student (EPFL)

Medical Robotics Technology Center
The Robotics Institute
Carnegie Mellon University
Pittsburgh, PA, USA

Robotics Research Centre &
Sch. of Mechanical & Aerospace Eng.
Nanyang Technological University
Singapore

Microsurgery with Active Handheld Instrument

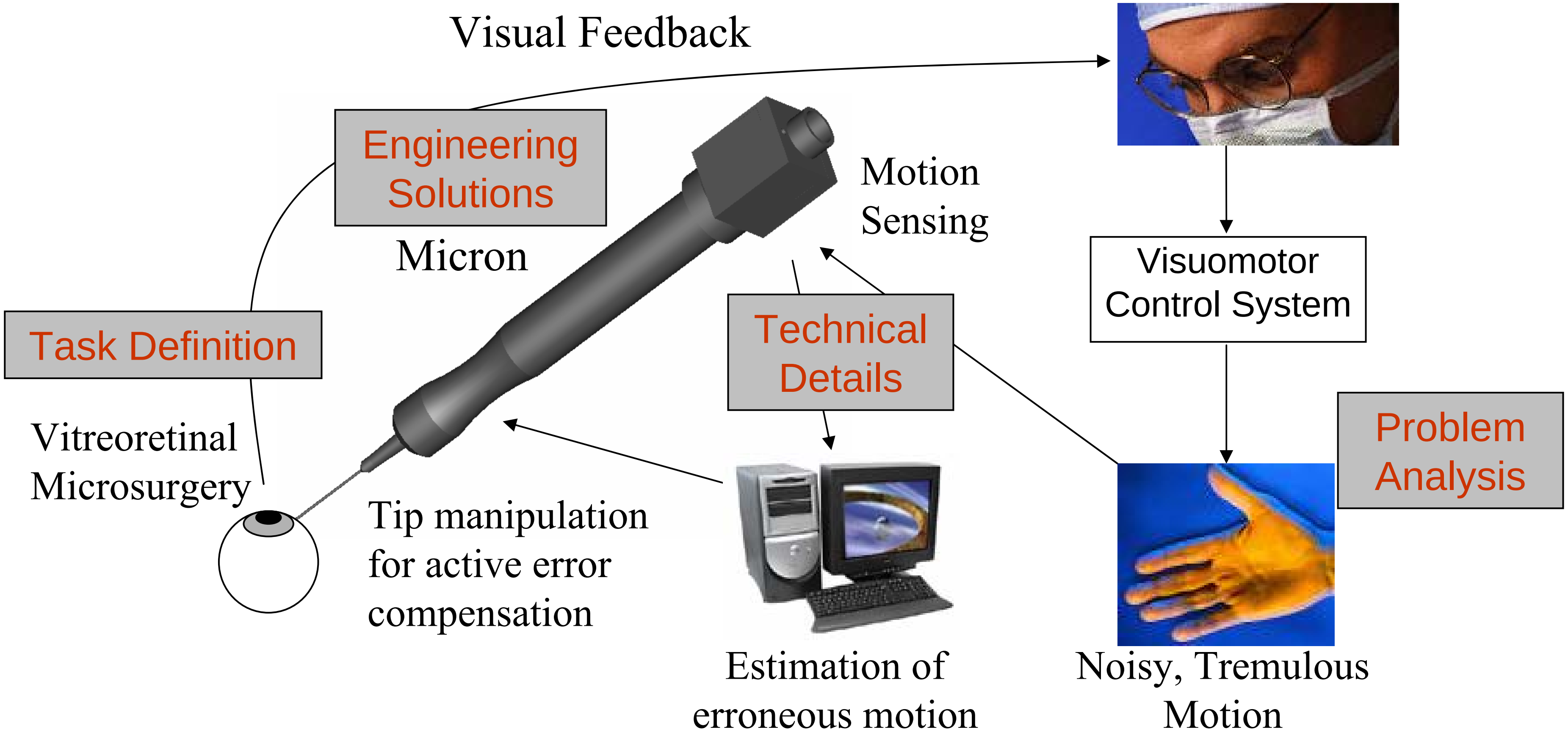

Vitreoretinal Microsurgery

- Removal of membranes ≤ 20 μm thick from front or back of retina

Vitreoretinal Microsurgery

- Injection of anticoagulant using intraocular cannulation to treat retinal vein (~∅100 µm) occlusion

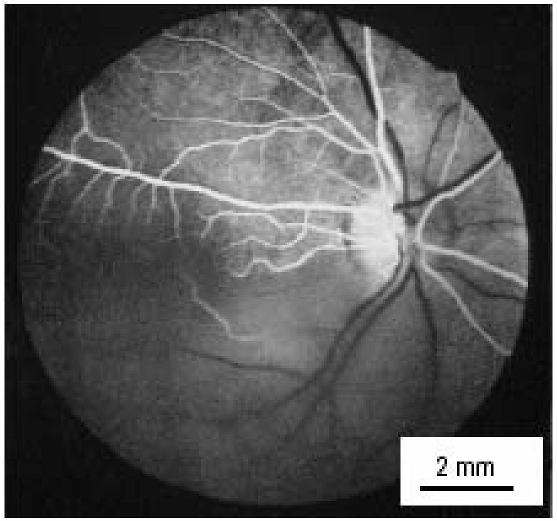

Retina with occluded retinal vein

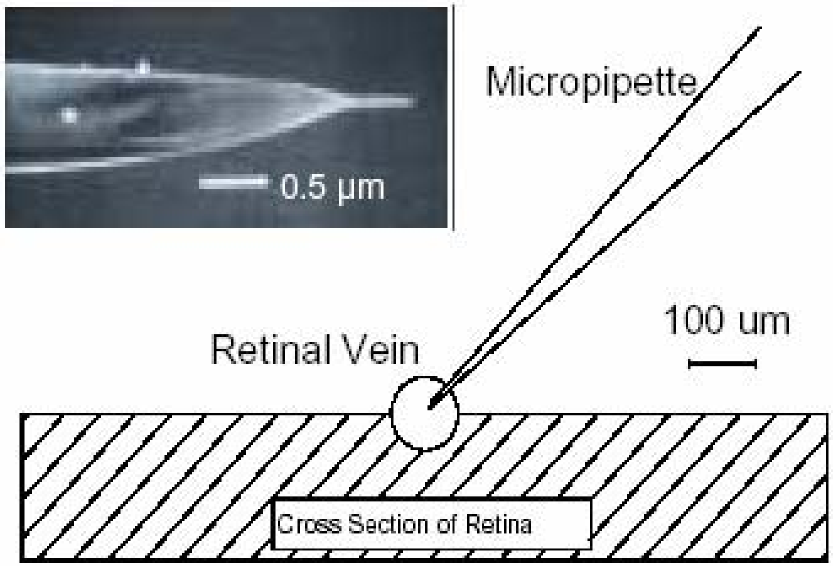

Vitreoretinal Microsurgery

- Tremor: under microscope

Involuntary Hand Movement and Microsurgery

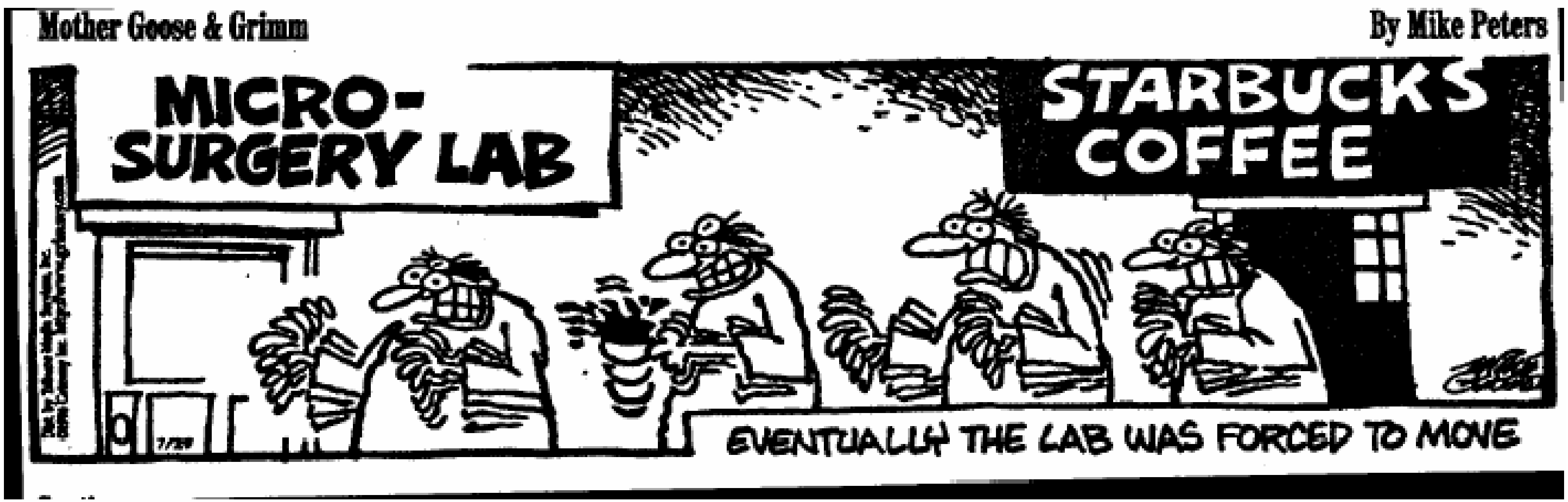

Involuntary Hand Movement and Microsurgery

- Complicate microsurgical procedures and makes certain delicate interventions impossible
- Impact on microsurgeons
  - 2 of 10 surgeons become microsurgeons
- Factors affecting tremor
  - Fatigue – strenuous exercise etc.
  - Caffeine/alcohol consumption
  - Lack of practice – long vacation etc.
  - Age – experience vs hand stability
- Microsurgeons' consensus:
  - 10 μm positioning accuracy

Involuntary Hand Movement of Healthy Human

- Physiological Tremor
  - Roughly sinusoidal motion, 8-12 Hz
  - ≤ 50 µm rms in each principal axis
- Non-tremulous Errors
  - Myoclonic jerk, drift etc.
  - Aperiodic, may be in the same frequency band as voluntary motion
  - Larger amplitude: > 100 µm

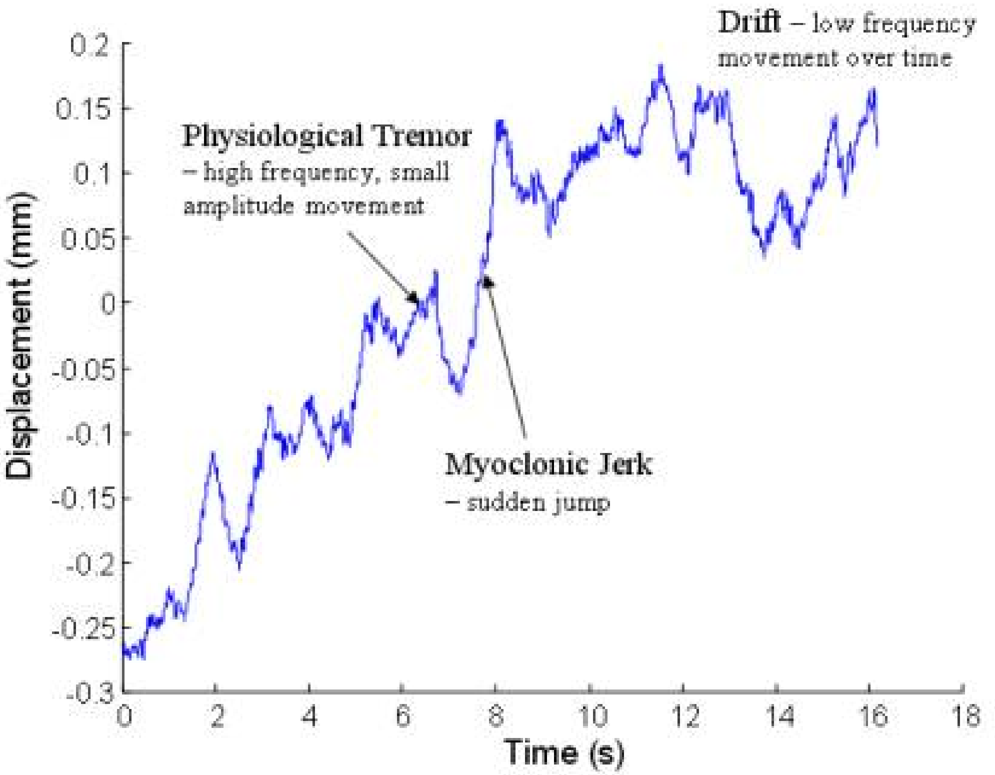

Microsurgery with Active Handheld Instrument

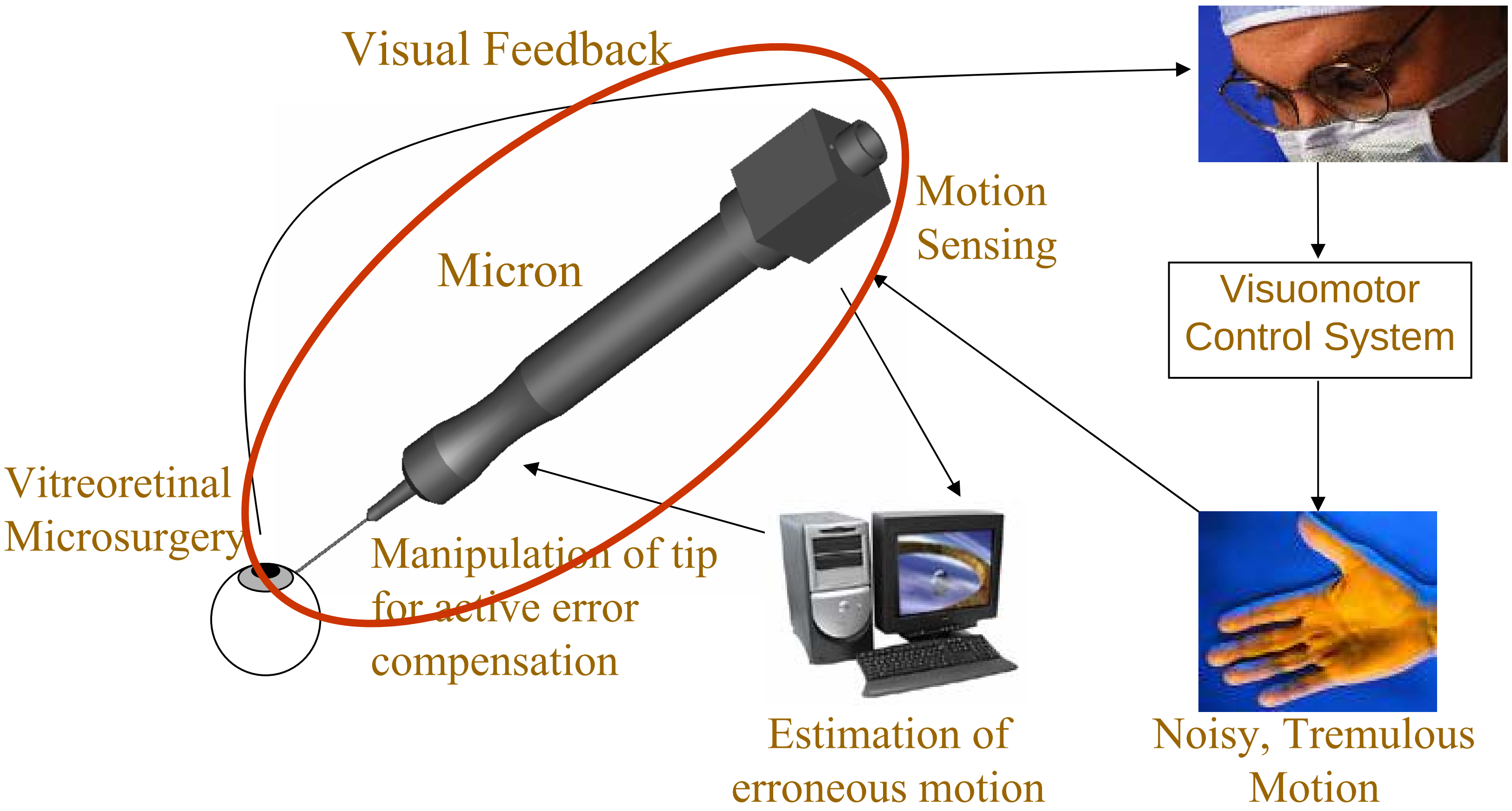

NANYANG TECHNOLOGICAL UNIVERSITY

Robotic Error Compensation Approaches

- Telerobotic systems: Zeus (Computer Motion) & Da Vinci (Intuitive Surgical)
  - Master-Slave manipulators
- Erroneous motion filtered by motion scaling

Computer Motion, Inc.

Robotic Error Compensation Approaches

- 'Steady-hand' robot:

  Russell Taylor et al., Johns Hopkins University
  - Surgeon and compliant robot hold tool simultaneously
  - Force feedback
  - 'Third hand' operation
- Erroneous motion damped by rigidity of robot

NANYANG TECHNOLOGICAL UNIVERSITY

Robotic Error Compensation Approaches

- Active Handheld Instrument:

  Paolo Dario, Scuola Superiore Sant'Anna, Pisa, Italy
- Same concept

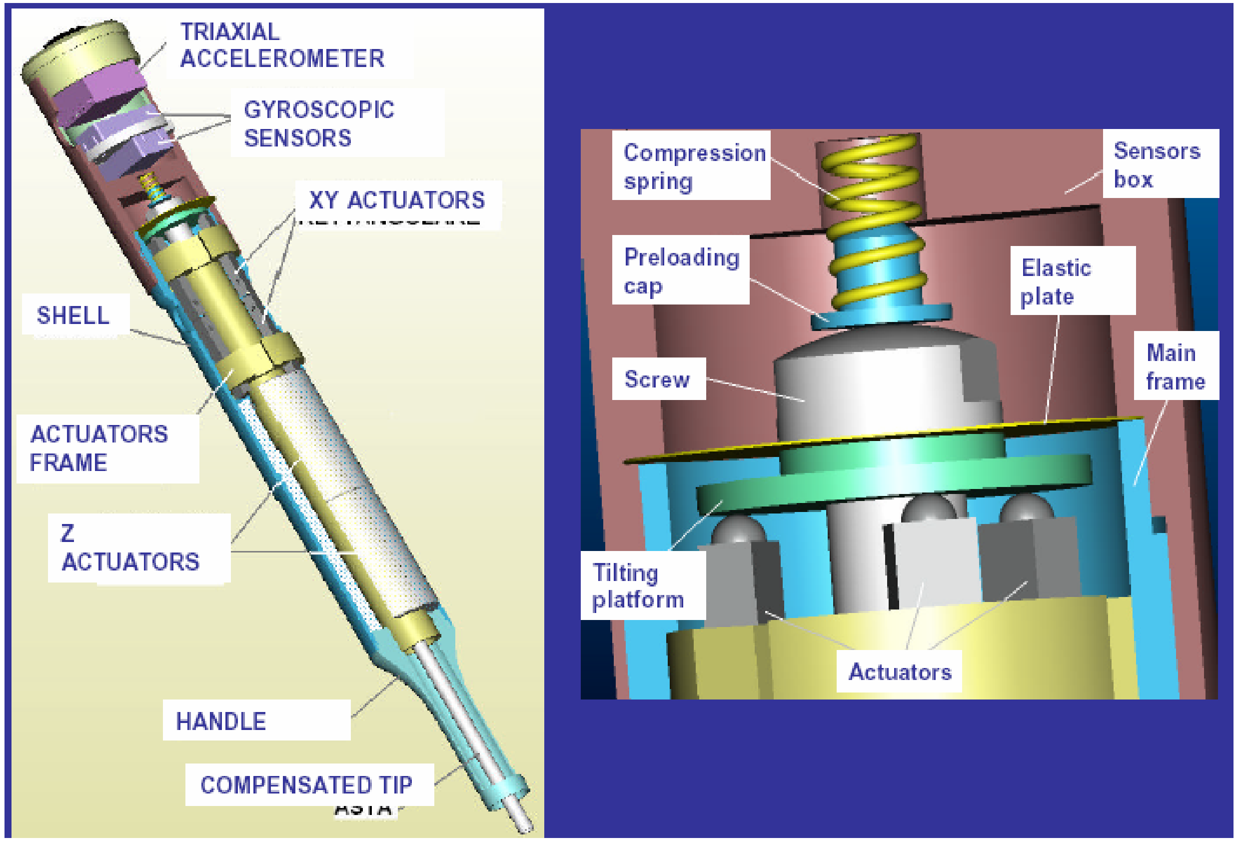

Comparison of Robotic Solutions

- Telerobotics
- 'Steady Hand' robot
- Active Handheld Instrument
  - ✓ Cheap
  - ✓ Unobtrusive
  - ✓ Safer
  - × Limited workspace
  - × No motion scaling
  - × No 'third hand'

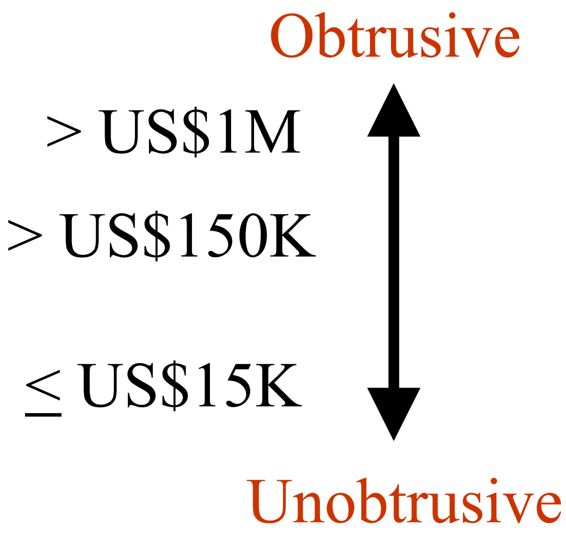

Micron Current Prototype

- Length: 180 mm long
- Diameter: Ø20(16) mm
- Weight <100 g
- 9 DOF inertial and magnetic sensing system at the back end
- 3 DOF piezoelectric driven parallel manipulator at front end with disposable surgical needle

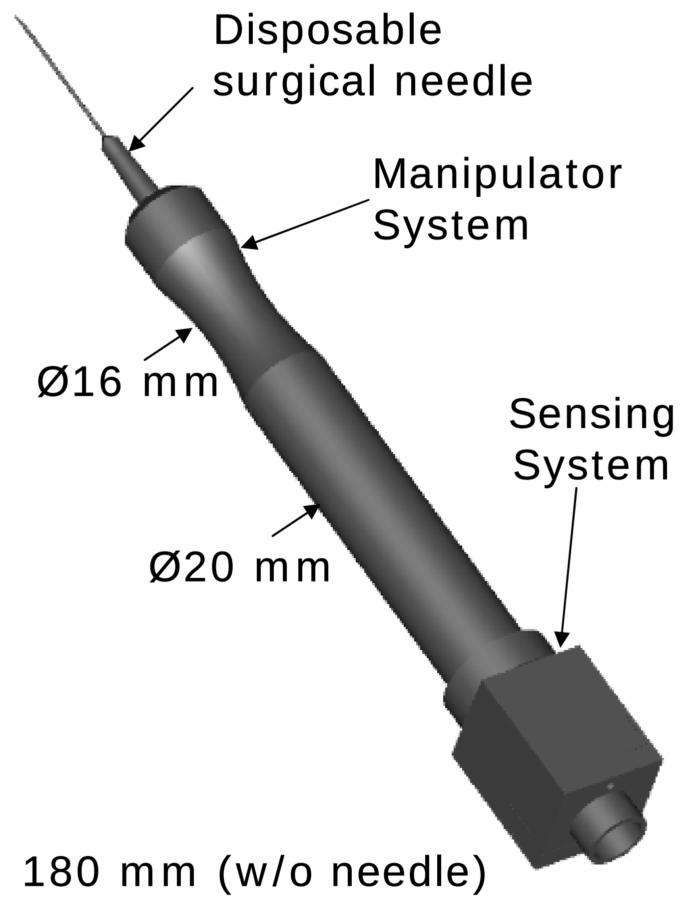

System Overview

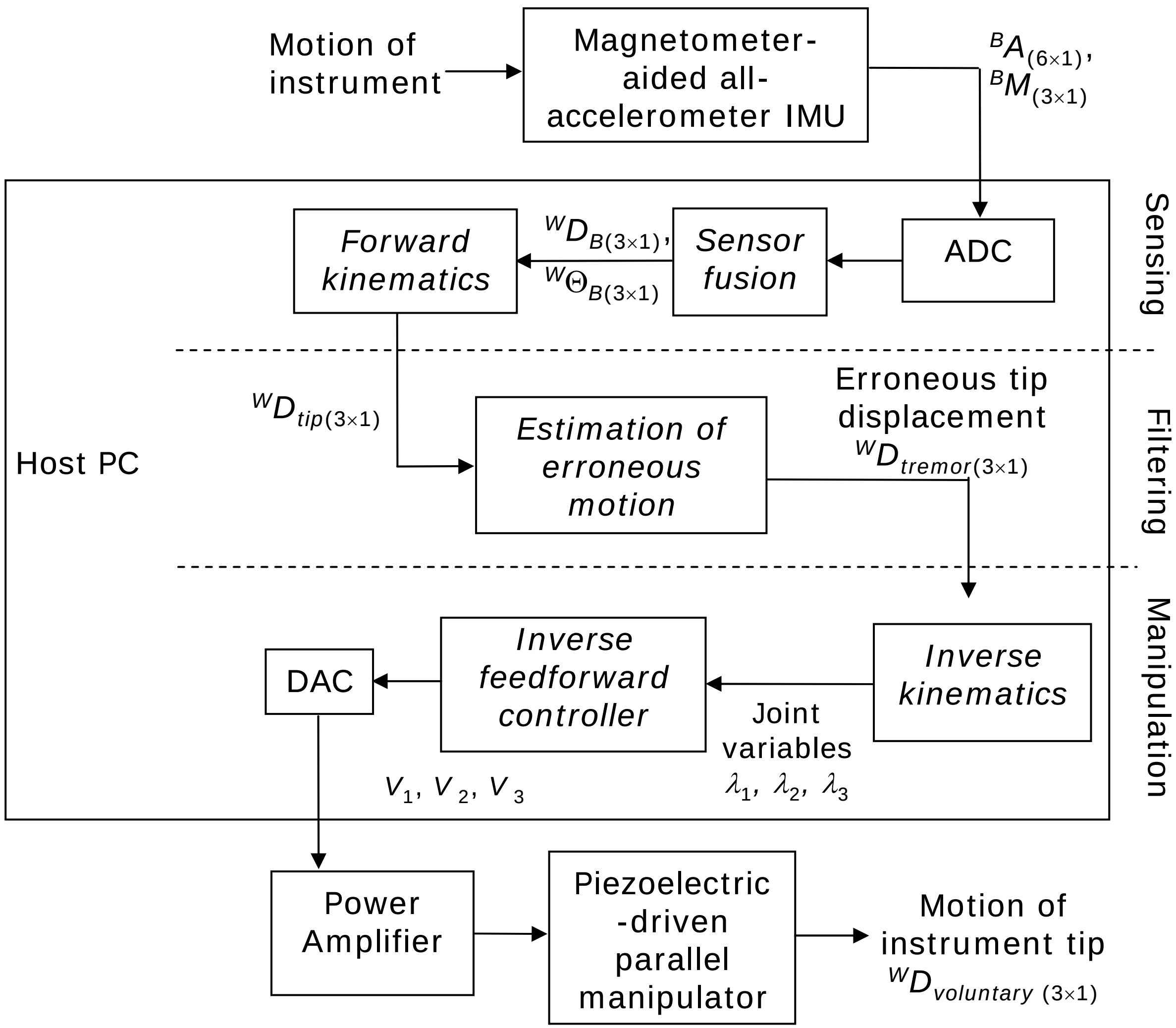

Microsurgery with Active Handheld Instrument

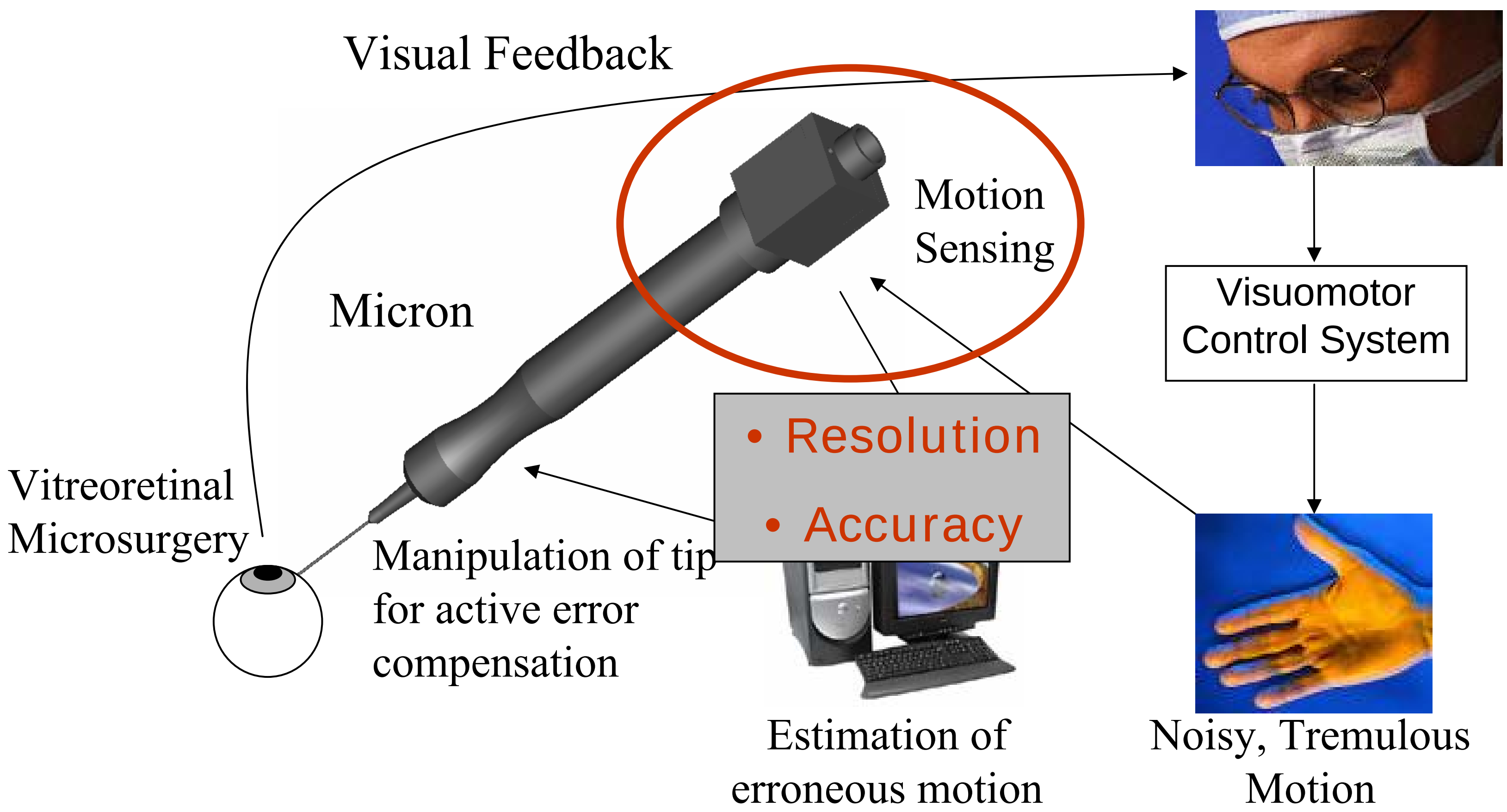

NANYANG TECHNOLOGICAL UNIVERSITY

Sensing System Design

- Magnetometer-aided all-accelerometer inertial measurement unit (IMU):
  - 3 dual-axis miniature MEMS accelerometers

    Analog Devices ADXL-203: 5mm x 5mm x 2mm, < 1g
  - Three-axis magnetometer

    Honeywell HMC-2003:

    26mm x 19mm x 12mm, <10g
- Housed in 2 locations

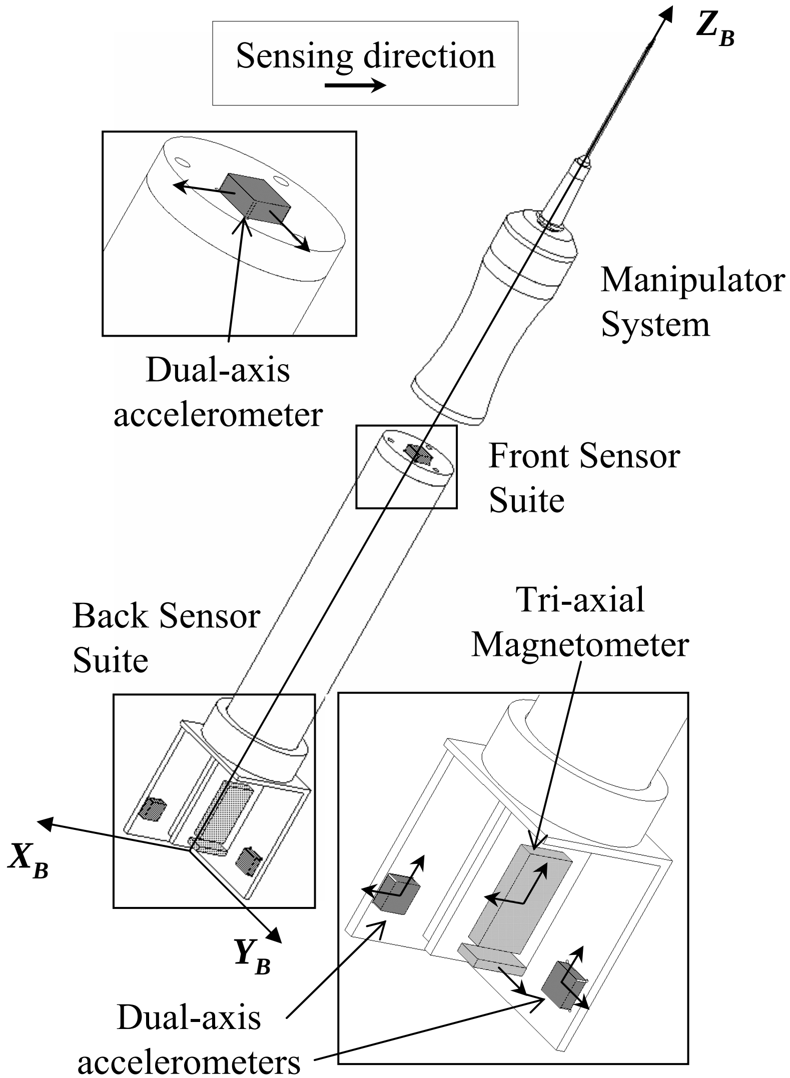

Sensing Modality

- Internally referenced sensors because:
  - Less obtrusive

    Externally referenced sensors require a line of sight
  - Resolution:

    Inertial sensor < 1 μm

    Externally referenced (e.g. Optotrak): ~ 0.1 mm
- All accelerometers because:
  - Low cost, miniature gyros too noisy

    $\rightarrow$ Poor sensing resolution
  - Navigation/tactical grade gyros - too expensive and bulky

Differential Sensing Kinematics

- Body acceleration sensed by accelerometer at location $\{i\}$:

Tangential Acceleration

$$A_i = A_{CG} + g + \underbrace{\Omega \times \Omega \times P_{Bi} + \dot{\Omega} \times P_{Bi}}_{\text{Rotation-induced Accelerations}}$$

Measurement

Centripetal Acceleration

- Differential Sensing

$$A_{ij} = A_j - A_i = \left([\Omega\times][\Omega\times] + [\dot{\Omega}\times]\right)P_{ij}, i, j = 1, 2, 3$$

$$A_{13} = \begin{bmatrix} a_{13x} \\ \bullet \\ \bullet \end{bmatrix}, A_{23} = \begin{bmatrix} \bullet \\ a_{23y} \\ \bullet \end{bmatrix}, A_{12} = \begin{bmatrix} \bullet \\ \bullet \\ a_{12z} \end{bmatrix}$$

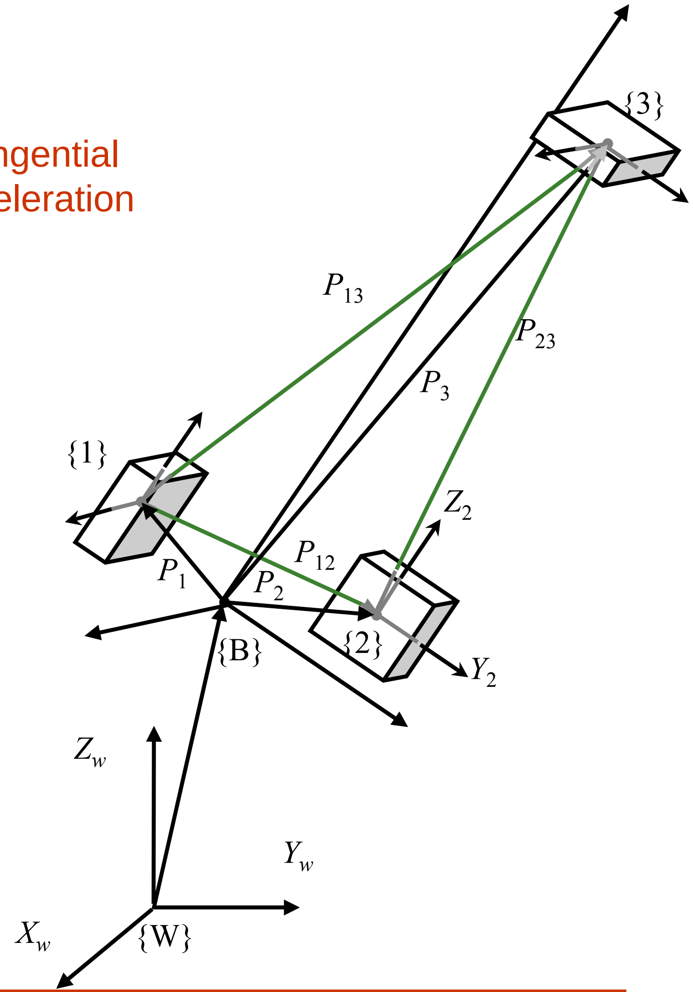

Differential Sensing Kinematics

- 3 unknowns:

  $\Omega = [\omega_x \ \omega_y \ \omega_z]^T$

  3 differential acceleration measurements:

  $A_D = [a_{13x} \ a_{23y} \ a_{12z}]^T$

- Solve system of nonlinear equations by Gauss-Newton or Levenberg-Marquart method
- Numerical instability
  - Assume $\Omega^2 \approx 0$, solve for $\dot{\Omega}$ analytically

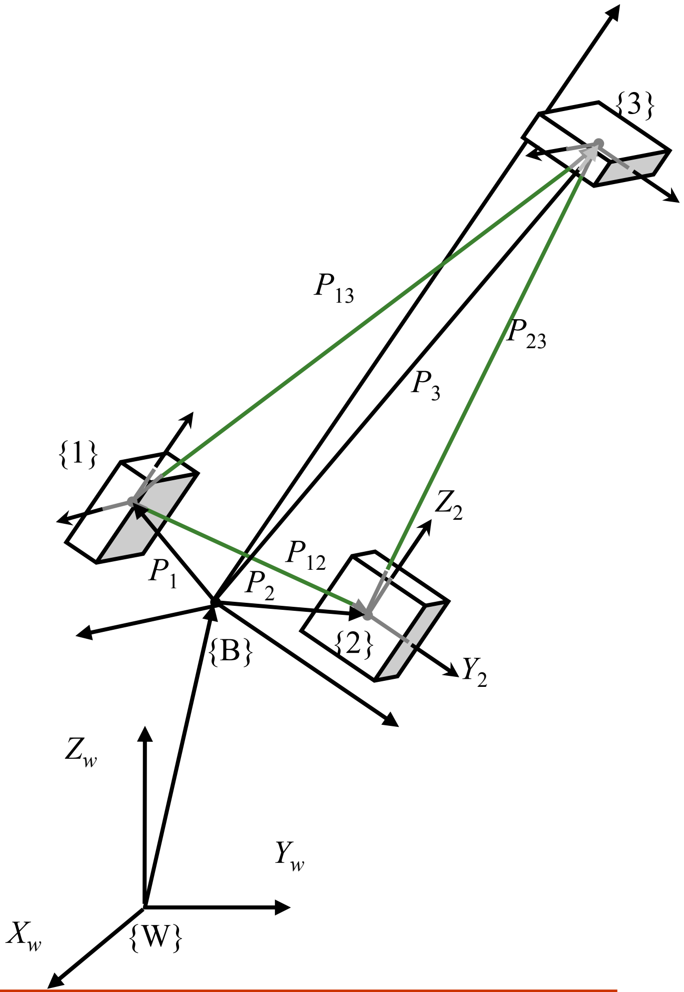

Sensing Kinematics

- Updating quaternions:

$$\dot{q}(t) = \tilde{\Omega}(t)q(t), \ \tilde{\Omega} = \frac{1}{2}\left[\begin{array}{c|c} [\Omega\times]_{3\times3} & \Omega_{3\times1} \\ \hline -\Omega_{1\times3}^T & 0 \end{array}\right]$$

- Directional Cosines matrix

$${}^{W}C_{B} = \begin{bmatrix} q_0^2 + q_1^2 - q_2^2 - q_3^2 & 2(q_1q_2 - q_0q_3) & 2(q_1q_3 + q_0q_2) \\ 2(q_1q_2 + q_0q_3) & q_0^2 - q_1^2 + q_2^2 - q_3^2 & 2(q_2q_3 - q_0q_1) \\ 2(q_1q_3 - q_0q_2) & 2(q_2q_3 + q_0q_1) & q_0^2 - q_1^2 - q_2^2 + q_3^2 \end{bmatrix}$$

- Gravity Removal: ${}^{W}A_{E} = {}^{W}C_{B}\,{}^{B}A - {}^{W}g$
- Tip Displacement:

$${}^{W}P_{tip}(t) = {}^{W}P_{tip}(t-T) + \int \int_{t-T}^{t} {}^{W}A_{E}(\tau)\,d\tau d\tau + {}^{W}C_{B}(t)[{}^{B}\Omega\times]^{B}P_{tip}$$

Sensing Resolution (Error Variance) Analysis

- Sensing resolution dependent on sensor noise floor
- Angular Sensing
  - Sensing equation:

    $$A_{ij} = f(\Omega) = ([\Omega\times]\,[\Omega\times] + [\dot{\Omega}\times])P_{ij}$$

  - Covariance:

    $$\mathrm{C}(A_{ij}) = \mathrm{C}(\Omega)\,P_{ij}$$

  - $P_{ij}\uparrow,\ \mathrm{C}(\Omega)\downarrow$

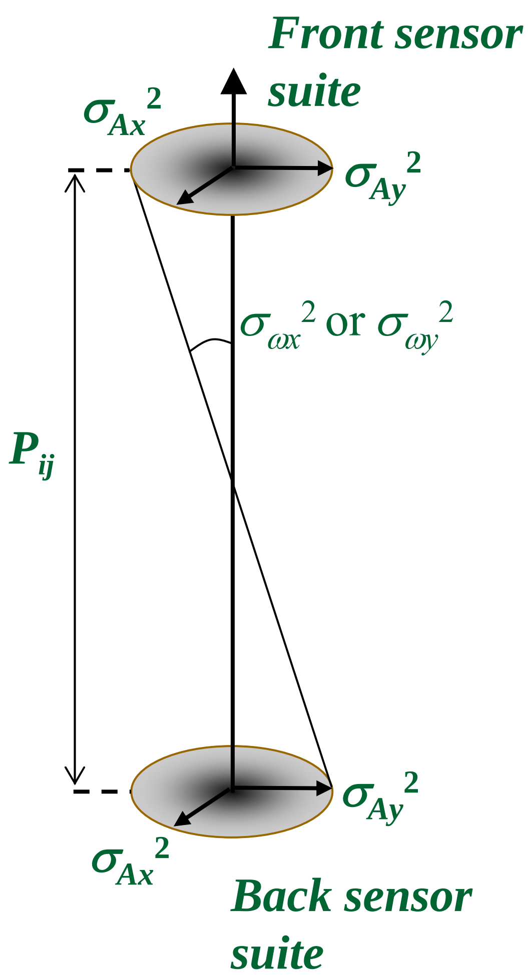

Proposed All-Accelerometer vs Conventional Inertial Measurement Unit

- All-accelerometer IMU
  - Maximized P_{ij}, with physical constraint of a slender handheld instrument
- Conventional IMU (3A-3G)
  - Tokin CG-L43D rate gyros x 3

	3G-3A Error std. dev. (deg/s)	6A Error std. dev. (deg/s)	Noise reduction / resolution improvement
ω_x & ω_y	1.41	1.08×10^{-2}	99.3% / 130x
ω_z	1.41	4.42×10^{-2}	96.9% / 32x

Angular Sensing Resolution Comparison

- Small angular velocity & sensor noise floor

Tokin Gyroscope

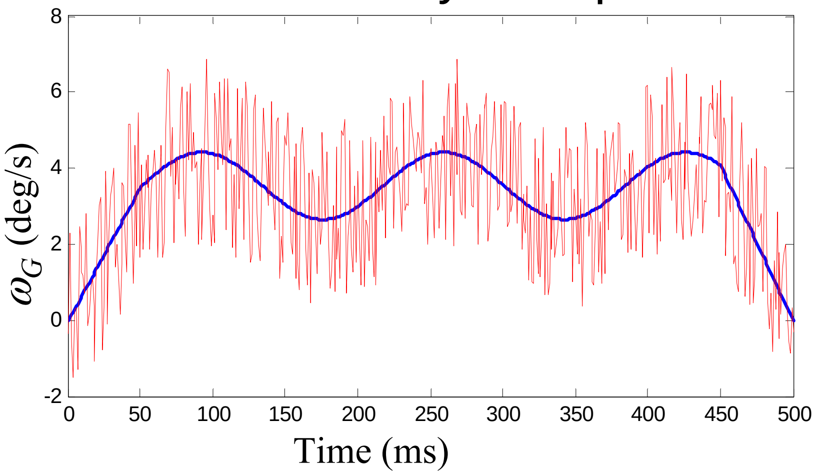

All-accelerometer IMU

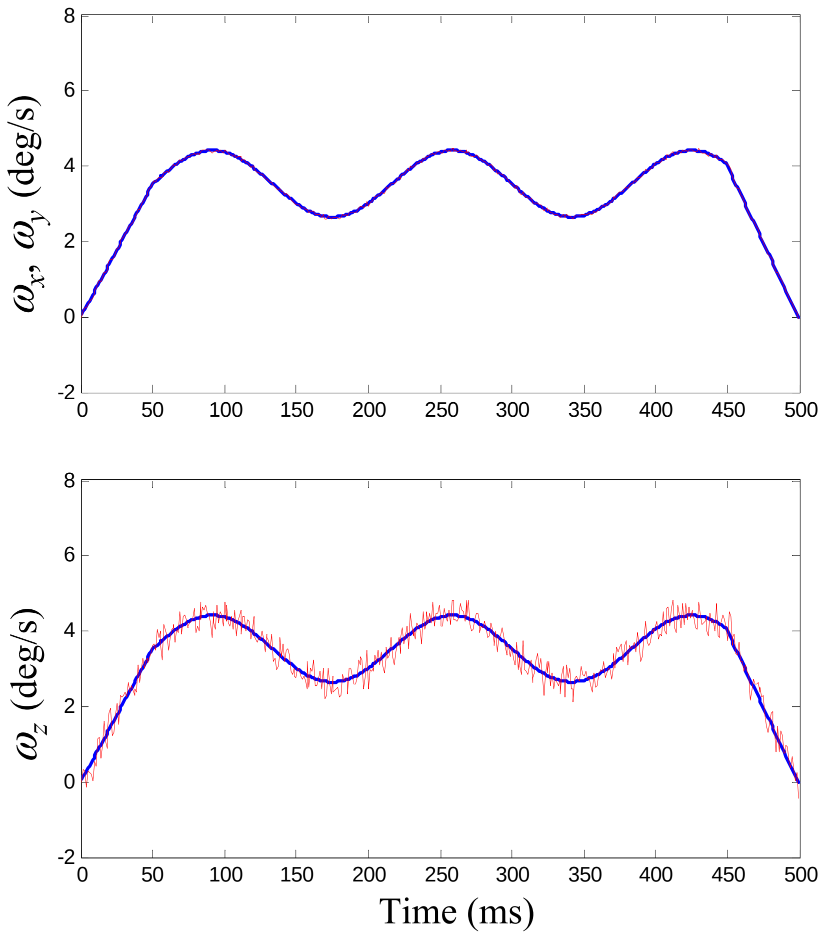

NANYANG TECHNOLOGICAL UNIVERSITY

Sensing Resolution (Error Variance) Analysis

- Translational Sensing
  - 2 accelerometers in each sensing direction:

$$\frac{1}{\sigma_A^2} = \frac{1}{\sigma_{Ai}^2} + \frac{1}{\sigma_{Aj}^2} \rightarrow \sigma_A = \frac{\sigma_{Ai}}{\sqrt{2}}$$

  - Sensing resolution improves by a factor of $2^{½}$
- Better orientation estimation $\rightarrow$ more complete removal of gravity $\rightarrow$ better translation estimation

Microsurgery with Active Handheld Instrument

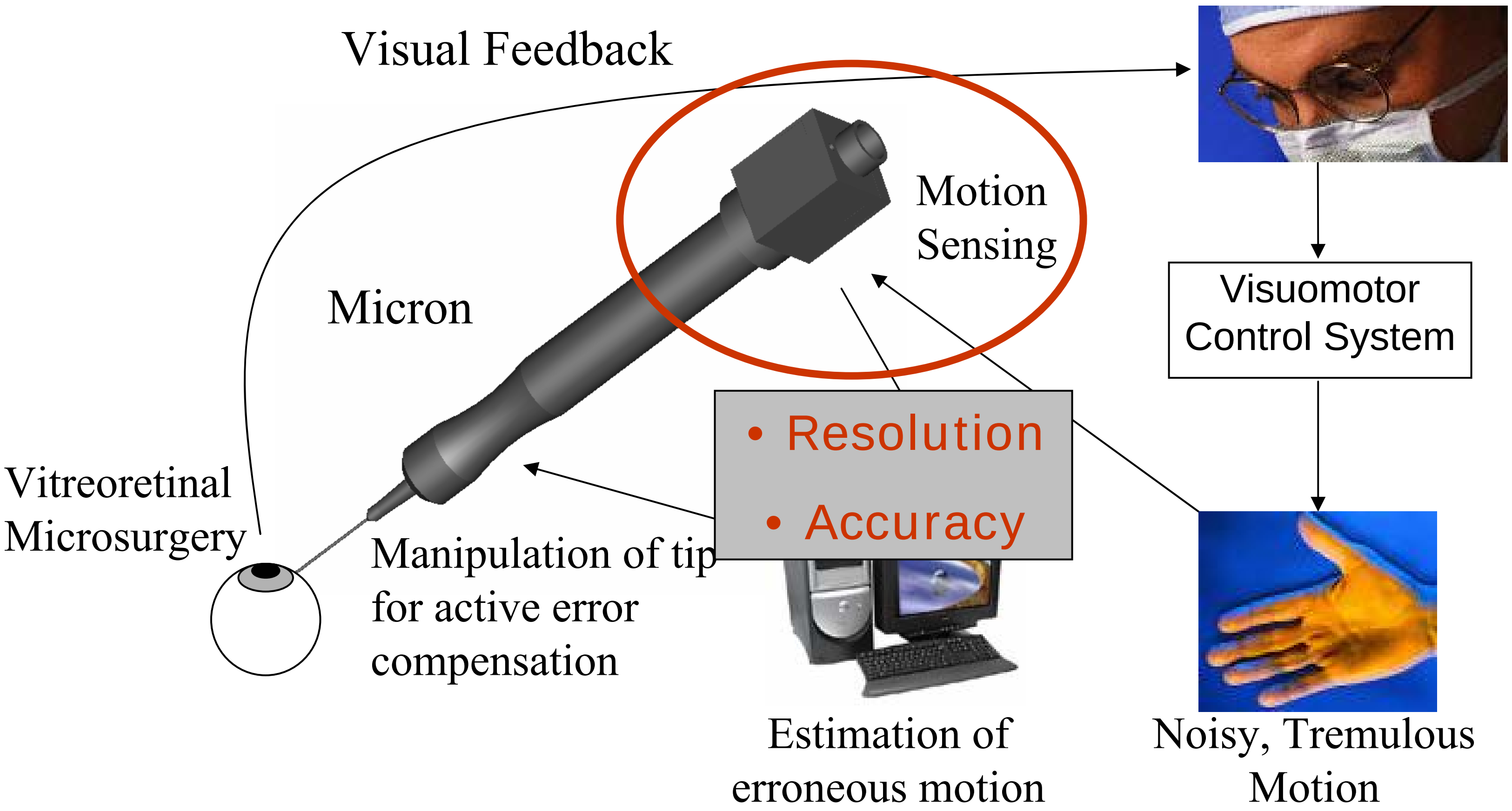

Integration Drift of Inertial Sensors

- Integration drift
  - Erroneous DC Offset $\xrightarrow{\int}$ Ramp $\xrightarrow{\int}$ Quadratic
  - Error accumulates and grows unbounded over time
- Poor sensing accuracy

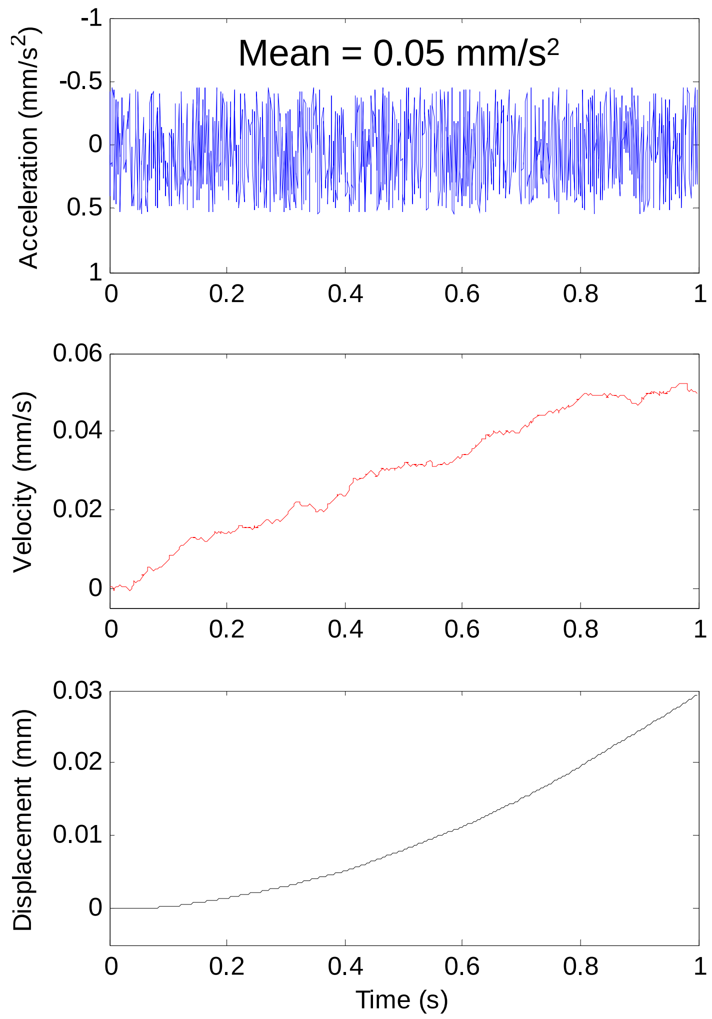

Measurement Model

- Measurement model allows error analysis and compensation
- Measurement Model = Physical (Deterministic) Model + Stochastic Model

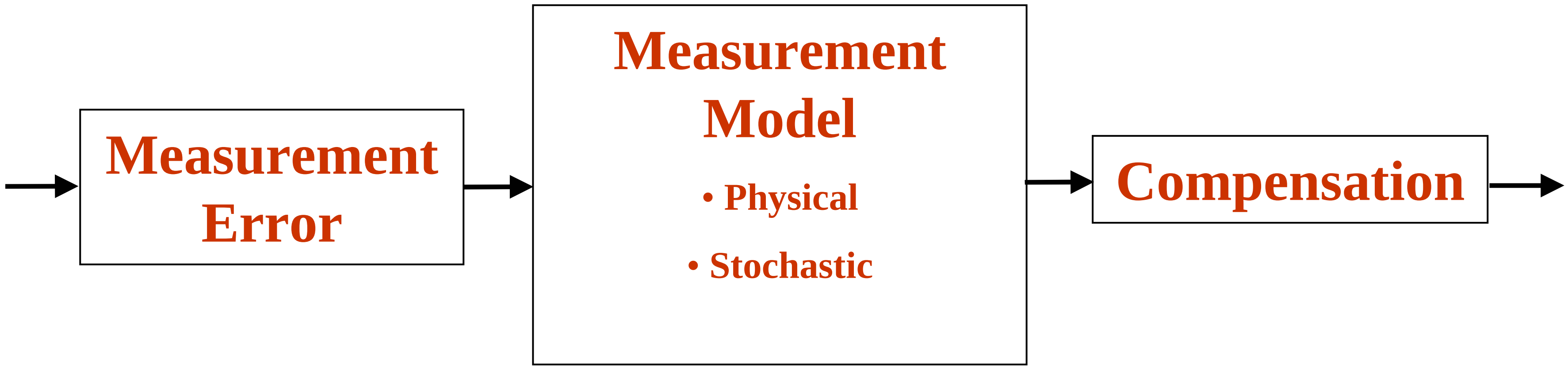

Accelerometer Model

- Calibration
  - Record accelerometer outputs at orientation inline (V_{+g}) and opposite (V_{-g}) to gravity
- Linear model
  - Acceleration,

    $A = (V_o - B)/SF \qquad g$
  - Scale factor,

    $SF = ½(V_{+g} - V_{-g}) \;\; \mathrm{V}/g$
  - Bias

    $B = ½\,(V_{+g} + V_{-g}) \quad \mathrm{V}$

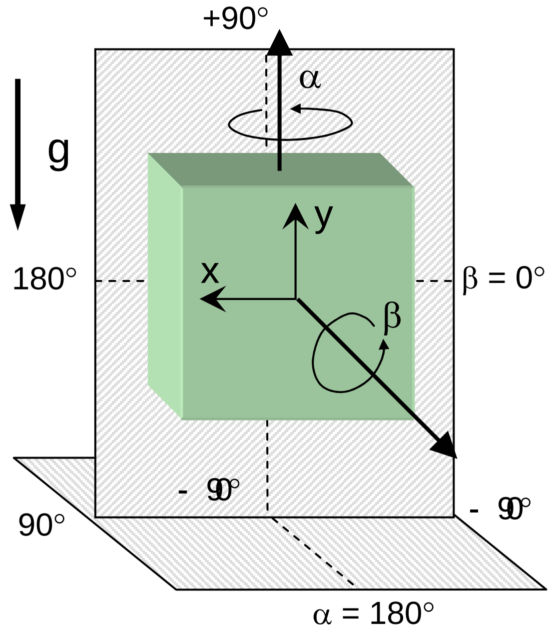

Experimental Observations

α = 90°, β = -180° to 180°

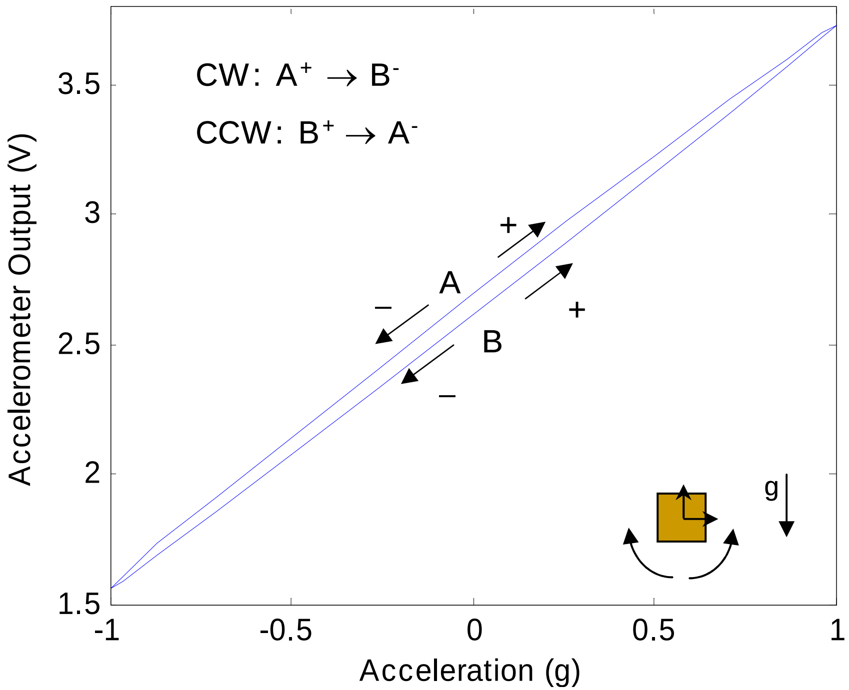

α = 30° & 150°, β = -180° to 180°

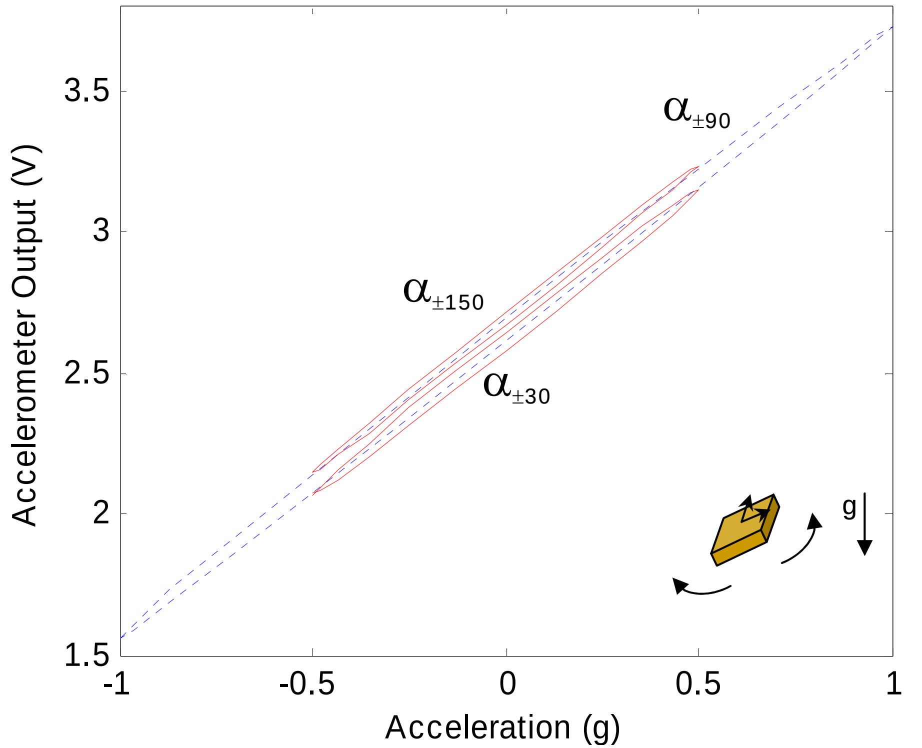

Phenomenological Modeling

- Bias, $B_x(V_y, V_z) = B_x + g_x(V_y) + h_x(V_z)$
- Scale Factor,

  $$SF_x(V_z) = r_{x2}V_z^2 + r_{x1}V_z + r_{x0}$$
- Model

$$A_x = (V_x - B_x(V_y, V_z)) / SF_x(V_z)$$

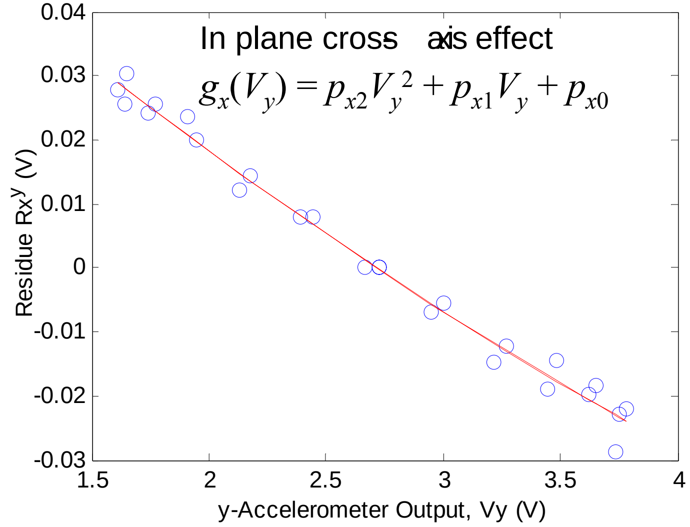

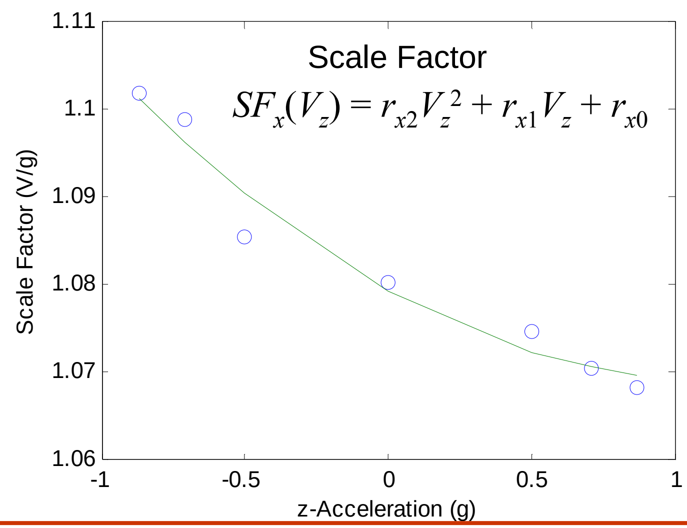

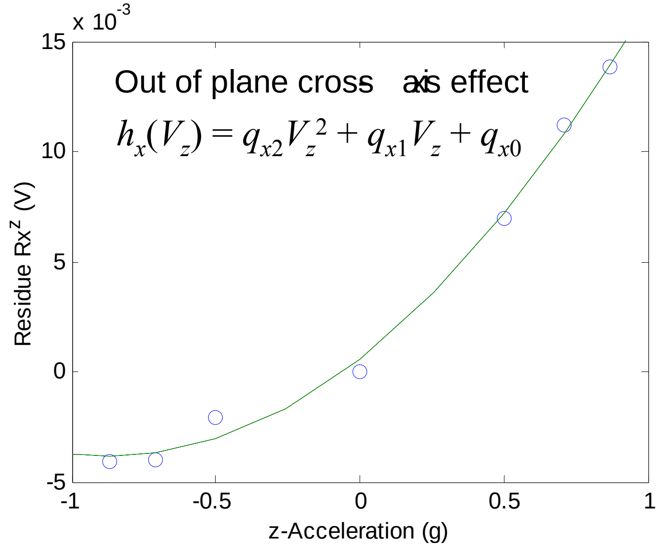

Sensing Experiment - Translation

- Motion generator
  - 10 Hz, 50 μm p-p sinusoid
- Displacement Sensor
  - Infrared interferometer (Philtec, Inc., Model D63)
  - Sub-micrometer accuracy

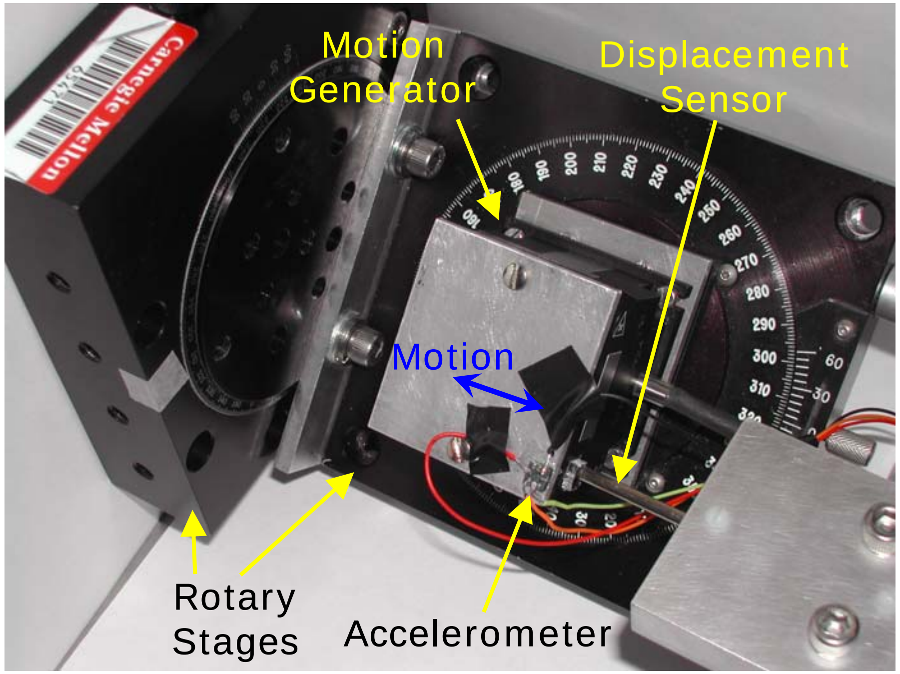

Sensing Results - Translation

	Rmse (mm/s^2)	Bias (mm/s^2)	Scale Factor (mm/s^2)
Linear Model	300	272	6
Proposed Physical Model	31*	<5	<1
Error Reduction (%)	89.7	-	-

* ADXL-203 rated rms noise = 22.1 mm/s^2

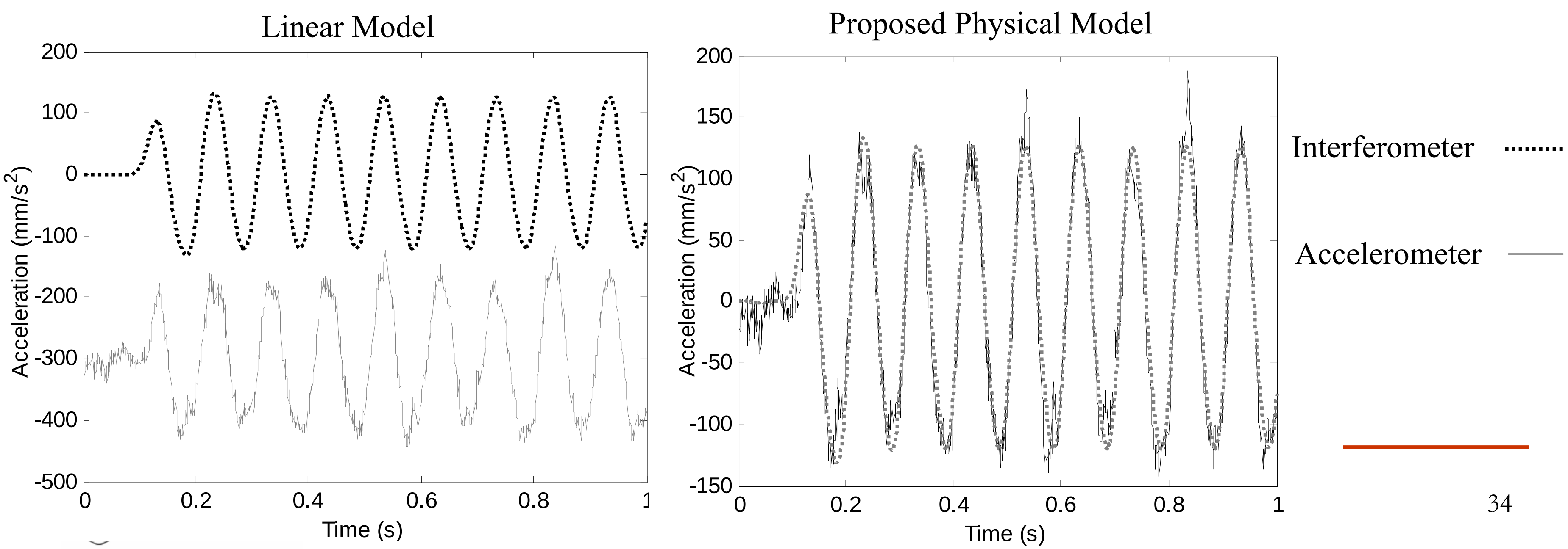

Stochastic Model

- Random noise analysis by Allan Variance method
- Dominant accelerometer noise types:
  - Velocity random walk
    - White noise in acceleration
  - Acceleration random walk
    - White noise in jerk
  - Trend / Bias Instability
    - Temperature drift

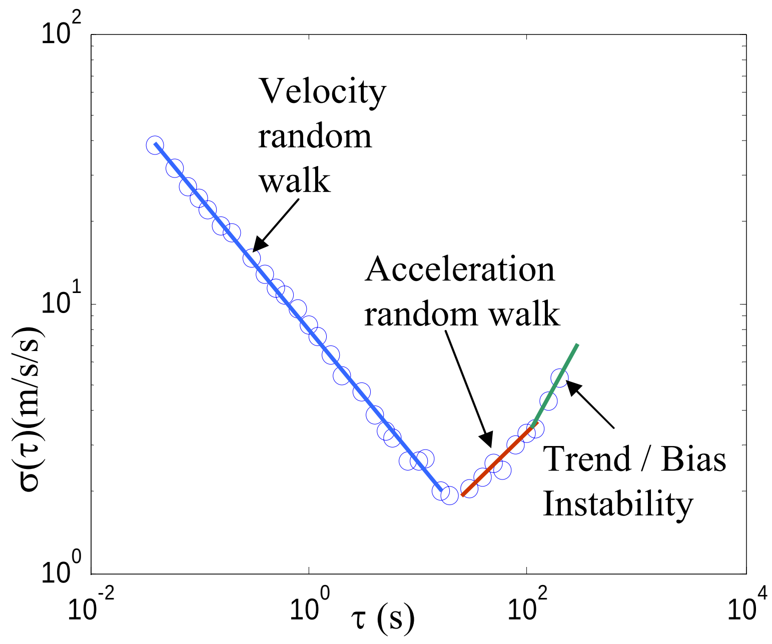

Temperature Drift

- Time varying zero bias
  - Heating up of internal circuitry
  - Steady state: 2-12 hours
- Solutions:
  - Modeling
  - Wait for steady state
  - Ovenization
    - Heat up sensor using power resistor
    - Changes sensor behavior

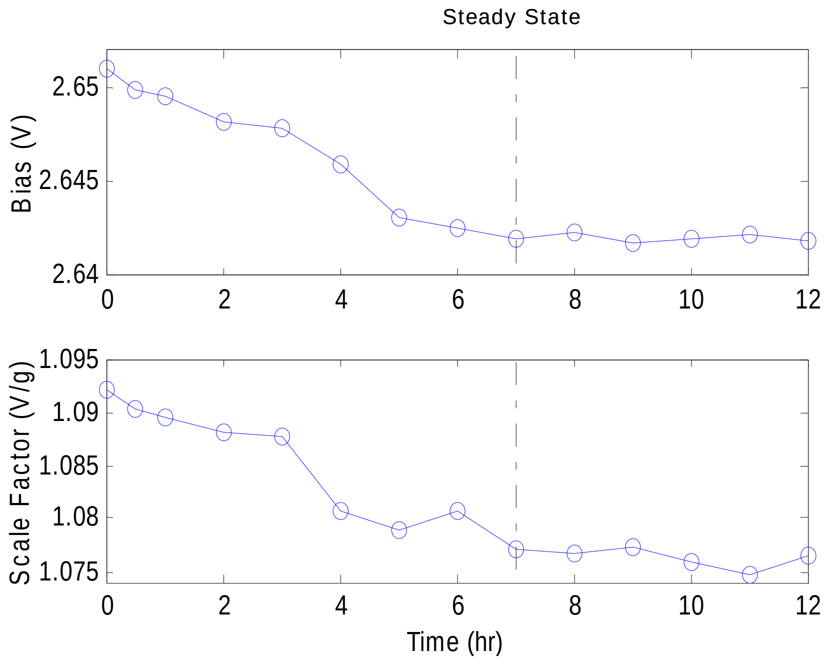

NANYANG TECHNOLOGICAL UNIVERSITY

Sensor Fusion via Cascaded Two-Stage Kalman Filtering

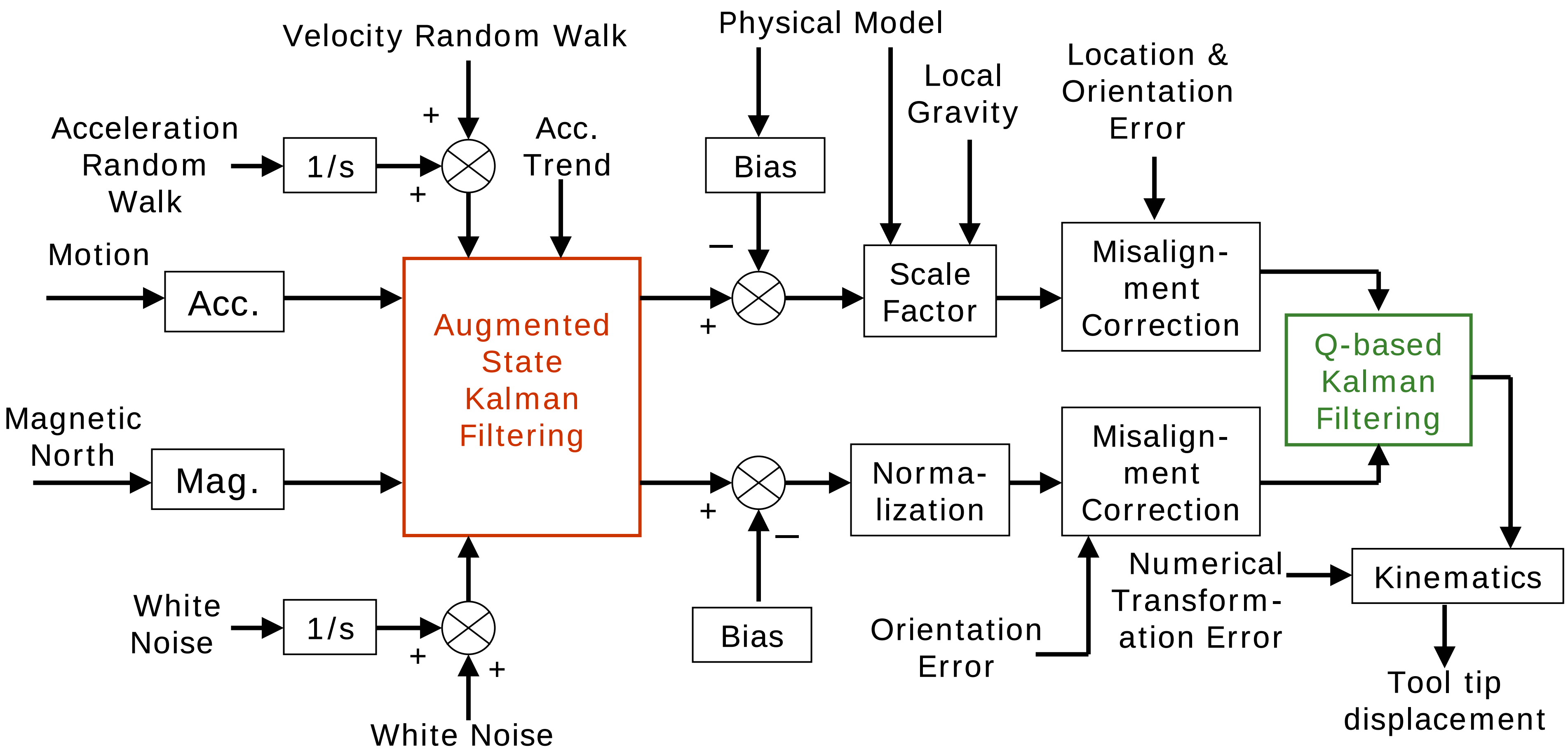

Augmented State Kalman Filtering

- Time domain sensor fusion
- Augmented state dynamic equation:

$$\underbrace{\begin{array}{c} \hat{x}\left\{\begin{matrix}\\ \\ \\ \end{matrix}\right. \\ \hat{b}\left\{\begin{matrix}\\ \\ \end{matrix}\right. \end{array}\begin{bmatrix} u[k+1] \\ a[k+1] \\ \dot{a}[k+1] \\ b_u[k+1] \\ b_a[k+1] \end{bmatrix}}_{x[k+1]} = \underbrace{\begin{bmatrix} 1 & T & \frac{1}{2}T^2 & 0 & 0 \\ 0 & 1 & T & 0 & 0 \\ 0 & 0 & 1 & 0 & 0 \\ 0 & 0 & 0 & 1 & T \\ 0 & 0 & 0 & 0 & 1 \end{bmatrix}}_{A} \underbrace{\begin{bmatrix} u[k] \\ a[k] \\ \dot{a}[k] \\ b_u[k] \\ b_a[k] \end{bmatrix}}_{x[k]} + \underbrace{\begin{bmatrix} 0 \\ 0 \\ 0 \\ 0 \\ c_1 T + c_2\left(2kT + T^2\right) \end{bmatrix}}_{c[k]} + \underbrace{\begin{bmatrix} 0 \\ \xi_{vrw}[k] \\ \xi_{arw}[k] \\ 0 \\ \beta[k] \end{bmatrix}}_{w[k]}$$

State Transition Matrix

Quadratic Model of Bias Drift

Velocity Random Walk

Acceleration Random Walk

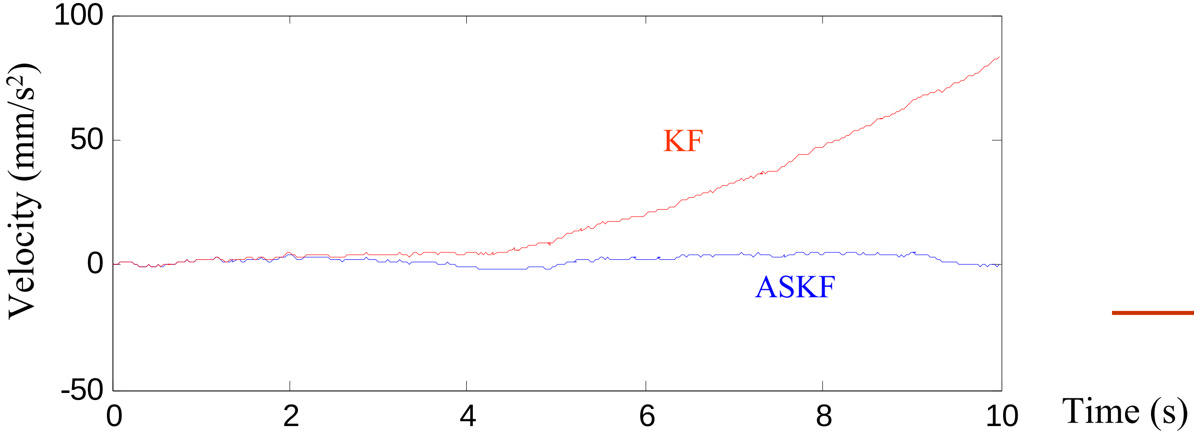

NANYANG TECHNOLOGICAL UNIVERSITY

Orientation Fusion

- Source 1: Differential sensing kinematics
  - $\Omega_A[k]$ from differential acceleration
  - State transition matrix:

$$F[k] = \cos\frac{\|\theta[k]\|}{2} I_{(4\times4)} + \frac{1}{\|\Omega[k]\|}\sin\frac{\|\theta[k]\|}{2}\tilde{\Theta}[k]_{(4\times4)}$$

$$\theta[k] = \Omega_A[k]T;\ \tilde{\Theta}[k] = \frac{1}{2}\left[\begin{array}{c|c} [\Omega_A\times]_{3\times3} & \Omega_{A3\times1} \\ \hline -\Omega_{A1\times3}^{T} & 0 \end{array}\right]T$$

  - Dynamic state equation: $q_A[k+1] = F[k]q_A[k] + \gamma[k]$
  - Orientation defined by quaternion
- + : high resolution

  – : drift

Orientation Fusion

- Source 2: TRIAD
  - Gravity vector & Magnetic North vector are non-collinear
  - TRIAD algorithm:
    - $z_B = -g_B / ||g||$;
    - $y_B = z_B \times N_B / || z_B \times N_B ||$;
    - $x_B = y_B \times z_B$
  - ${}^{W}C_B = [x_B \ \ y_B \ z_B]$
- + : non-drifting

  – : poor resolution

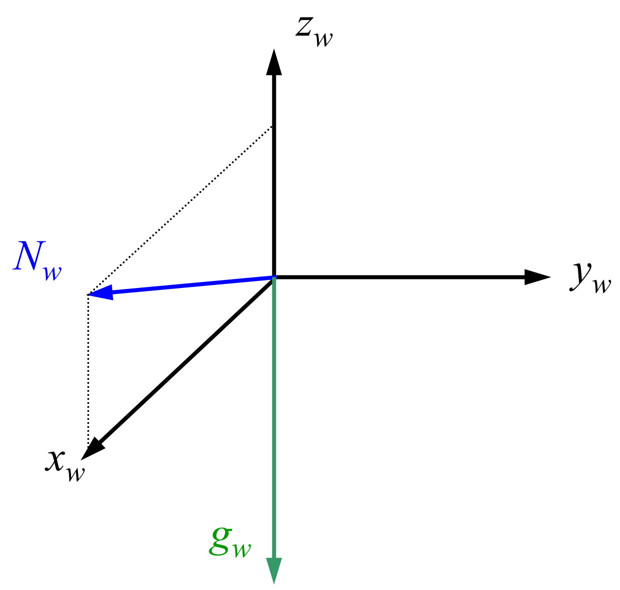

Quaternion-based Kalman Filtering - Gravity Tracking

- Source 1: Ω_A
  - High resolution, drifting
- Source 2: $N_B + g_B$
  - Noisy, non-drifting
- Quaternion-based KF: Q-KF
  - Reduced noise, non-drifting

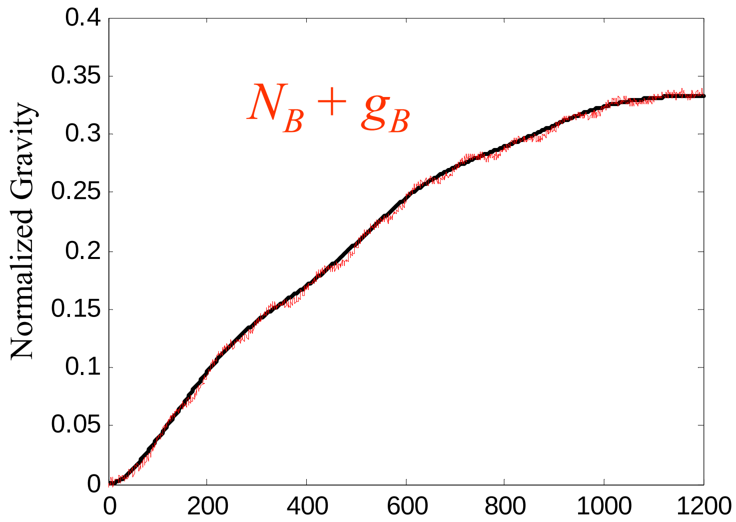

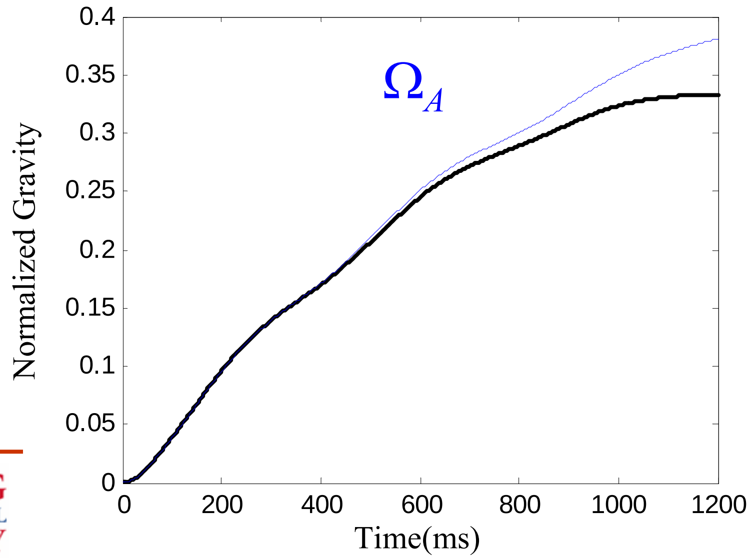

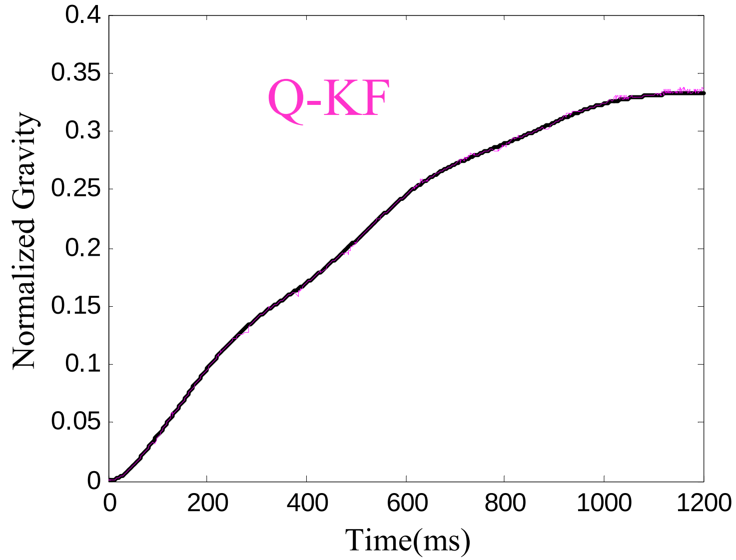

Sensing Experiment - Orientation

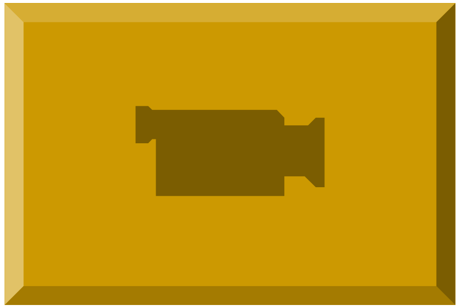

Translational Sensing Accuracy

- No non-drifting reference
  - Poor translational sensing accuracy
- Not important if tremor is separable from drift and intended motion

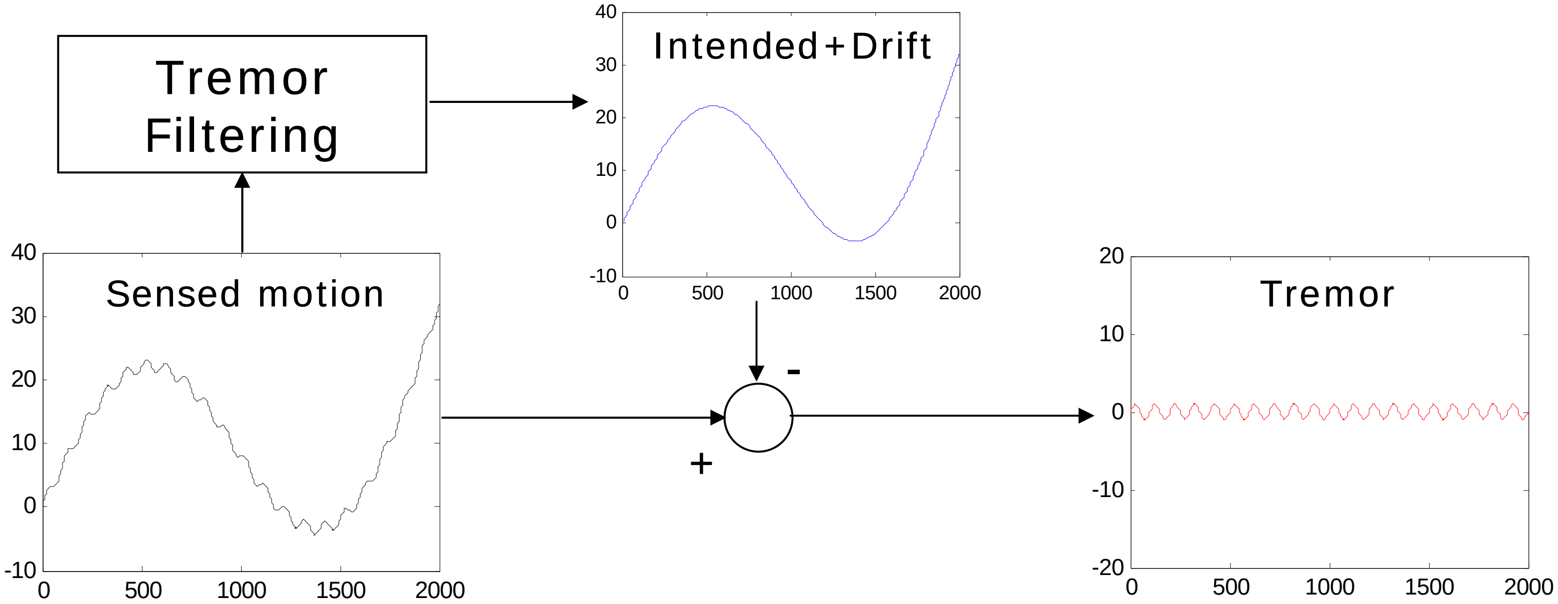

NANYANG TECHNOLOGICAL UNIVERSITY

Microsurgery with Active Handheld Instrument

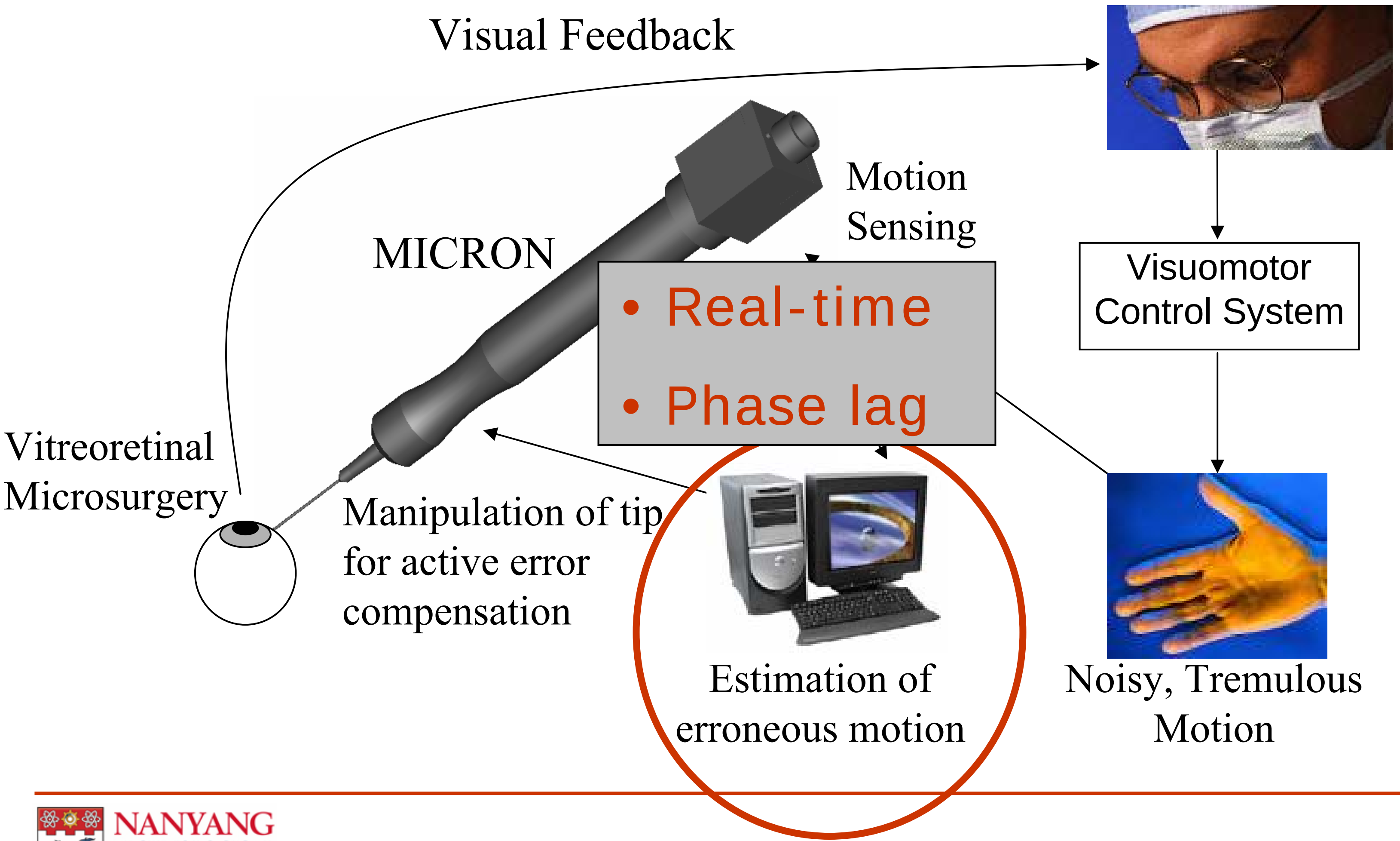

Frequency Selective Filters Phase Characteristics

- Physiological tremor has a distinct frequency bands:8 – 12 Hz
  - Voluntary motion: $\leq$ 1 Hz; Electrical noise: >> 12 Hz
- Classical frequency selective bandpass / band-stop (notch) filters
  - Phase lag $\equiv$ Group (time) delay
  - Filtered signal is a time delayed version of the actual sensed motion
  - Unacceptable condition for real-time error canceling application: compensating action might worsen the error

Zero Phase Filtering

- Separation of tremor from the intended motion without introducing phase lag
  - Prediction/projection capability
  - Adaptive
    - Non-linear phase response of IIR filter, i.e. phase characteristic changes with frequency
- Two proposed algorithms
  - Weighted-frequency Fourier Linear Combiner (WFLC)
  - Adaptive Phase Compensating Band-pass Filter

Fourier Linear Combiner (FLC)

- Truncated Fourier series to adaptively estimate amplitude and phase of periodic signal with *known frequency* (ω_0)

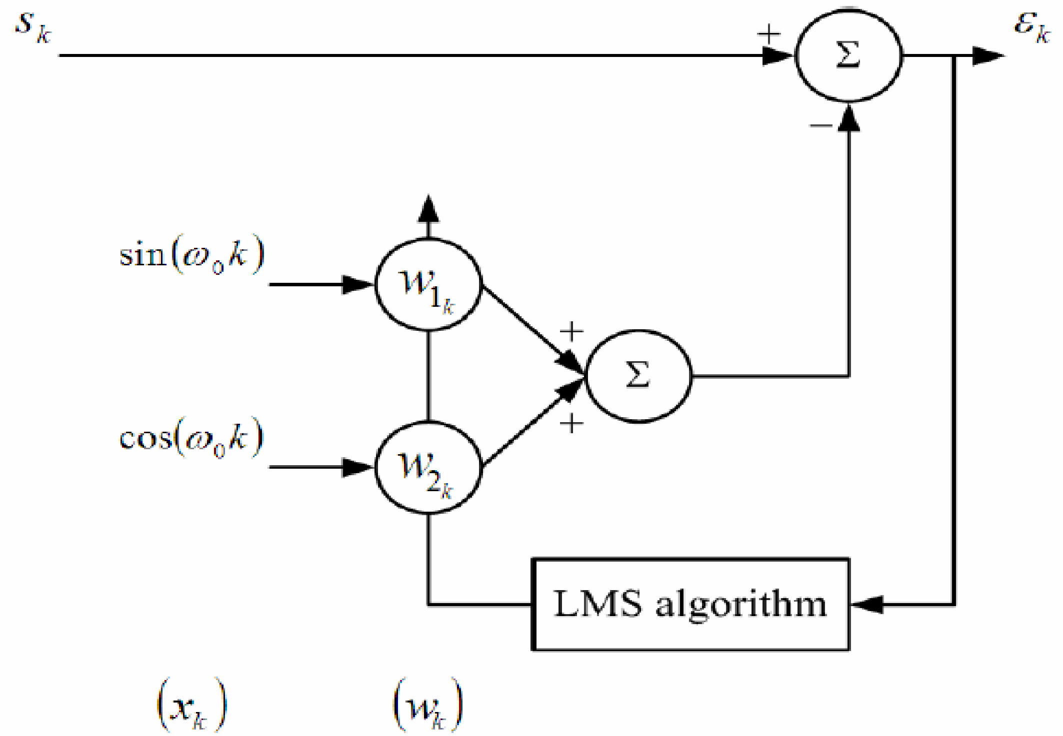

Weighted-frequency Fourier Linear Combiner (WFLC)

- Extends FLC to also adaptively estimate the frequency using another LMS algorithm
- Band-pass filter to select the band of interest
  - Assumption: rate of change of the dominant input signal frequency is slow
- Zero-phase notch (band-stop) filter effect

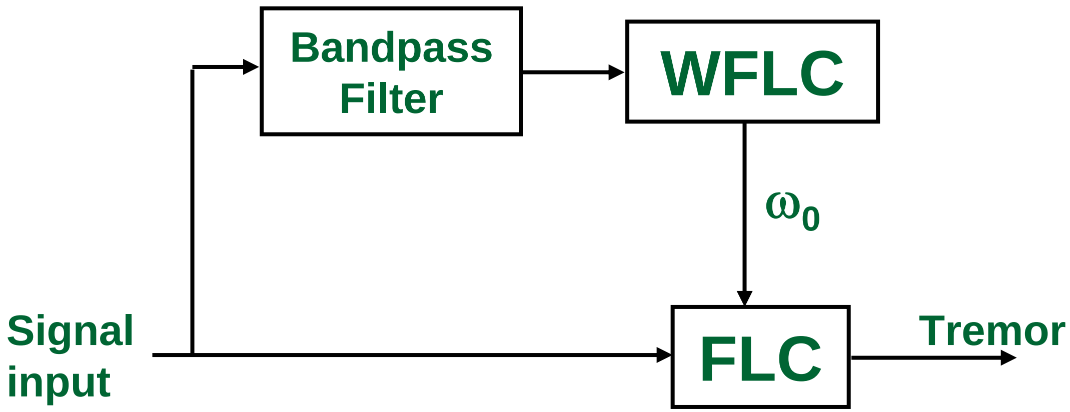

Weighted-frequency Fourier Linear Combiner (WFLC)

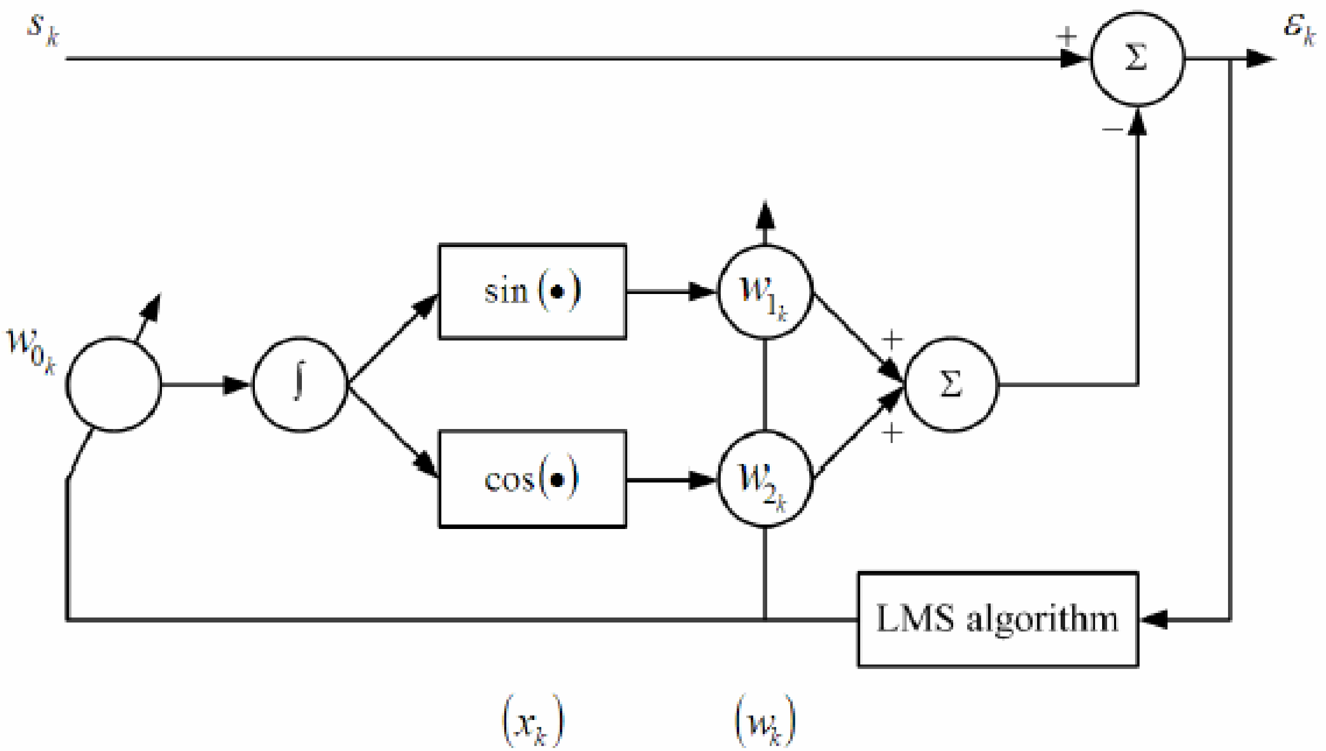

Weighted-frequency Fourier Linear Combiner (WFLC) Experiment

- 1 DOF motion canceling experiment
- Ave. rms tremor amplitude reduced 69%
- Stability problem
  - Double adaptive algorithm

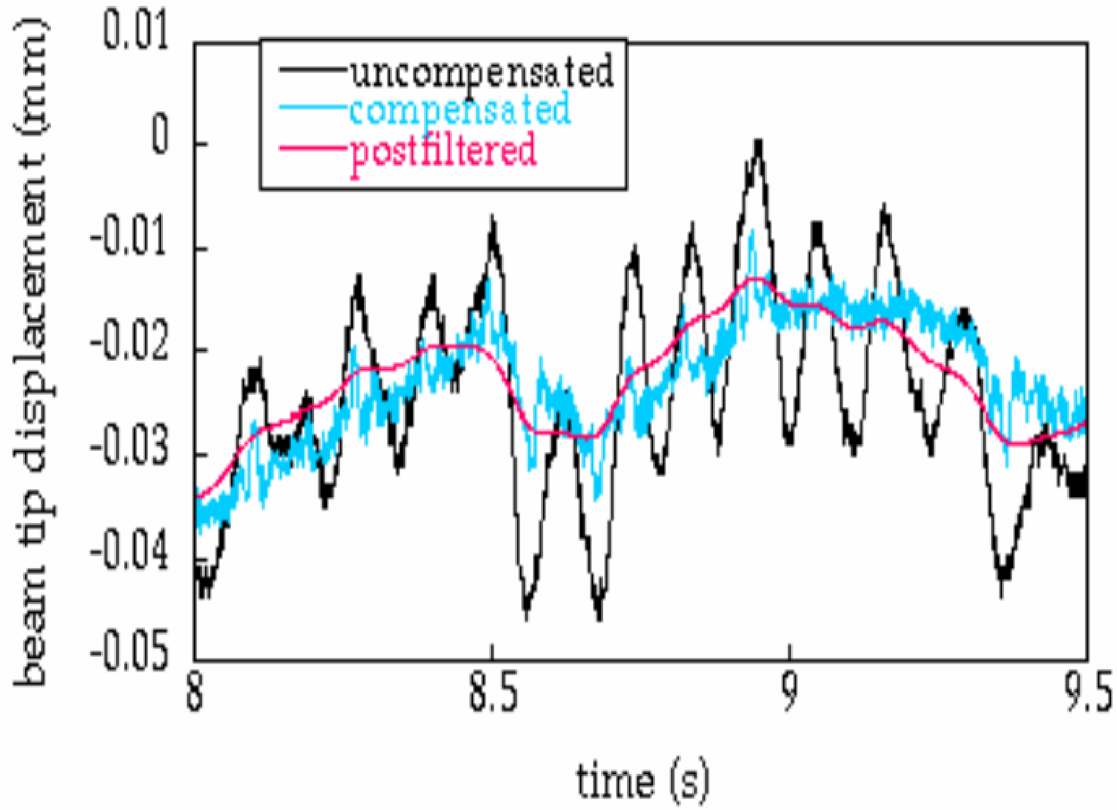

Filter Phase Characteristics

- Low-pass filters create phase *lag*
- High-pass filters create phase *lead*

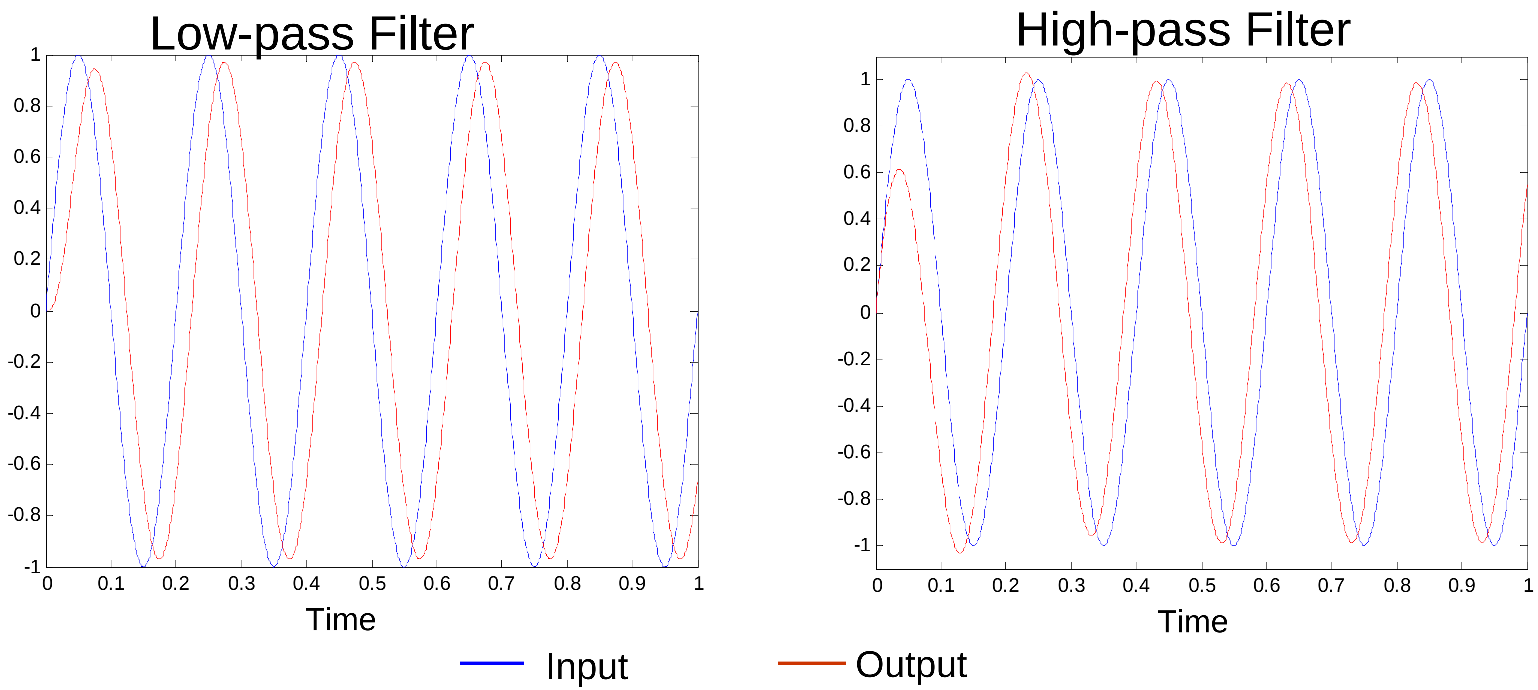

Adaptive Phase Compensating Band-pass Filter

- The idea:
  - To design a cascaded low-pass and high-pass filters such that phase lag of low-pass is compensated by phase lead of high-pass for a certain known input frequency
  - WFLC to estimate the instantaneous frequency
- Motivation
  - Most sensors come with built-in low pass filters

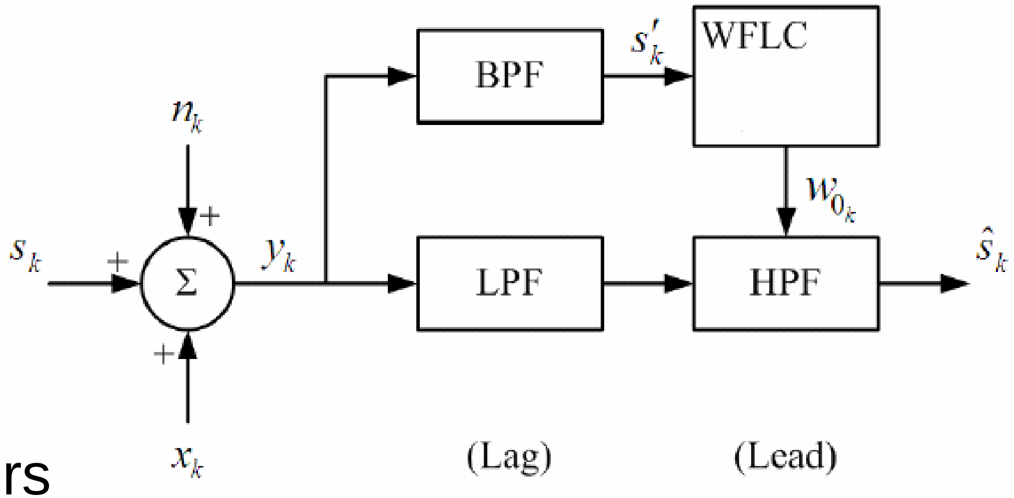

Implementation

- Design LP-HP filter pairs with equal and opposite phase characteristics
- Filter design frequency band: 3 – 7 Hz
- Filter type: Elliptical 2nd order
- Roots of transfer function can be modeled by a linear function

Roots of Filter Transfer Functions

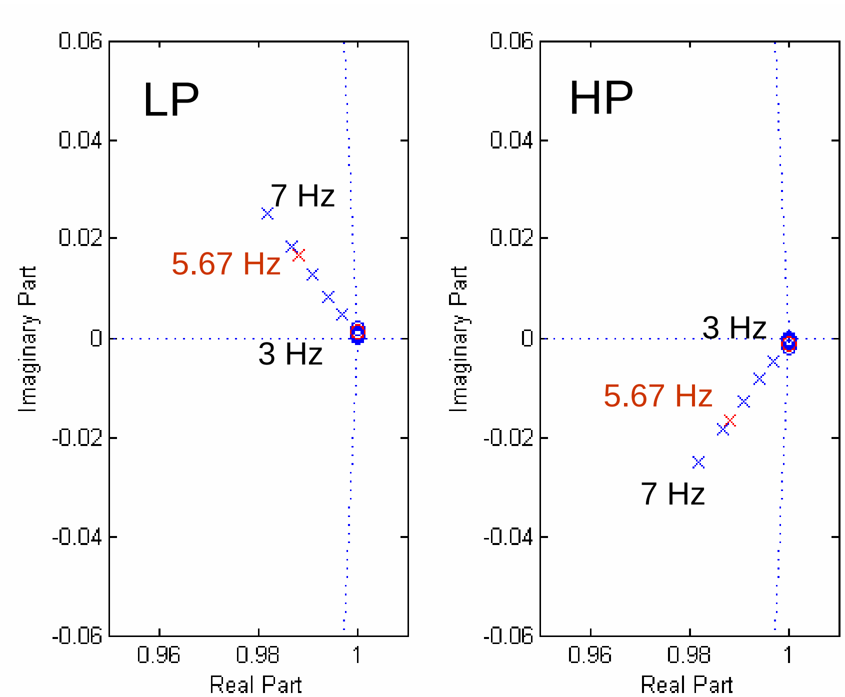

× - Poles   o - Zeros

Adaptive Phase Compensating Band-pass Filter

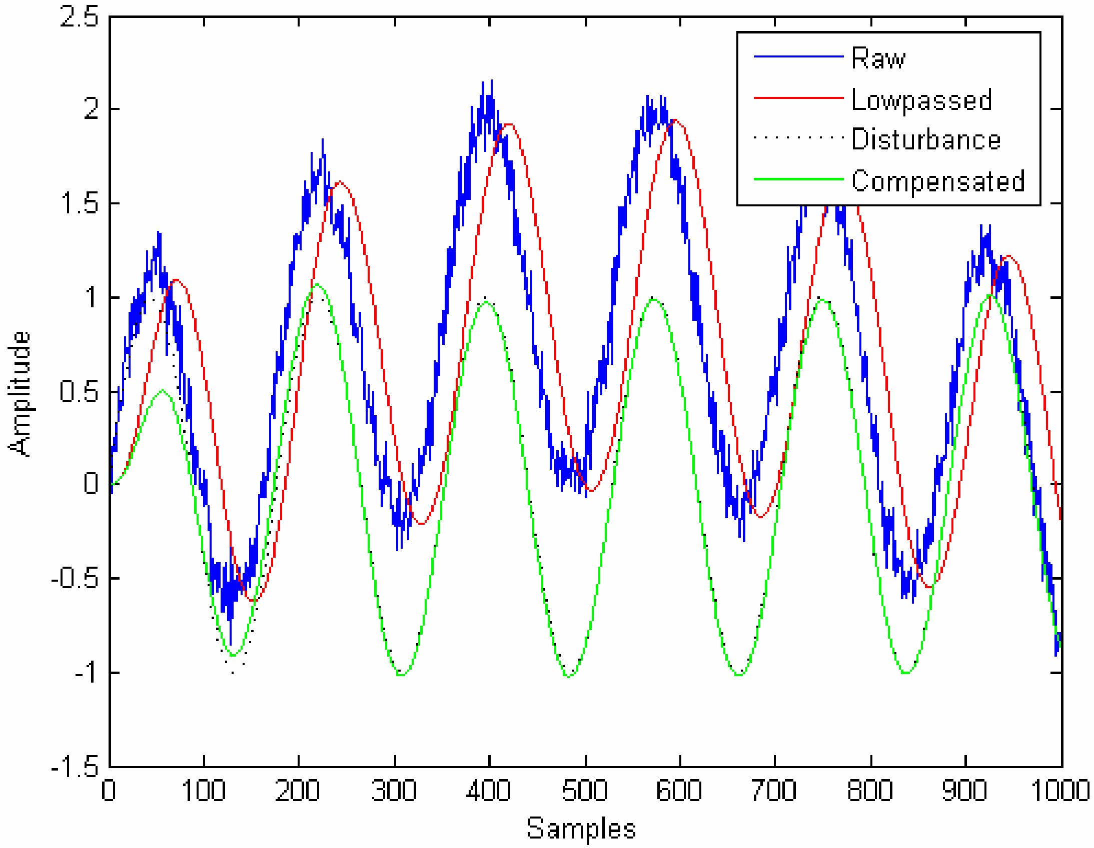

NANYANG TECHNOLOGICAL UNIVERSITY

Motion Canceling Experiment

- Motion generator oscillating at 2.0 Hz
- Camcorder recording a rectangular target
  - 25 frames per second
- Image post processing to simulate real-time compensation

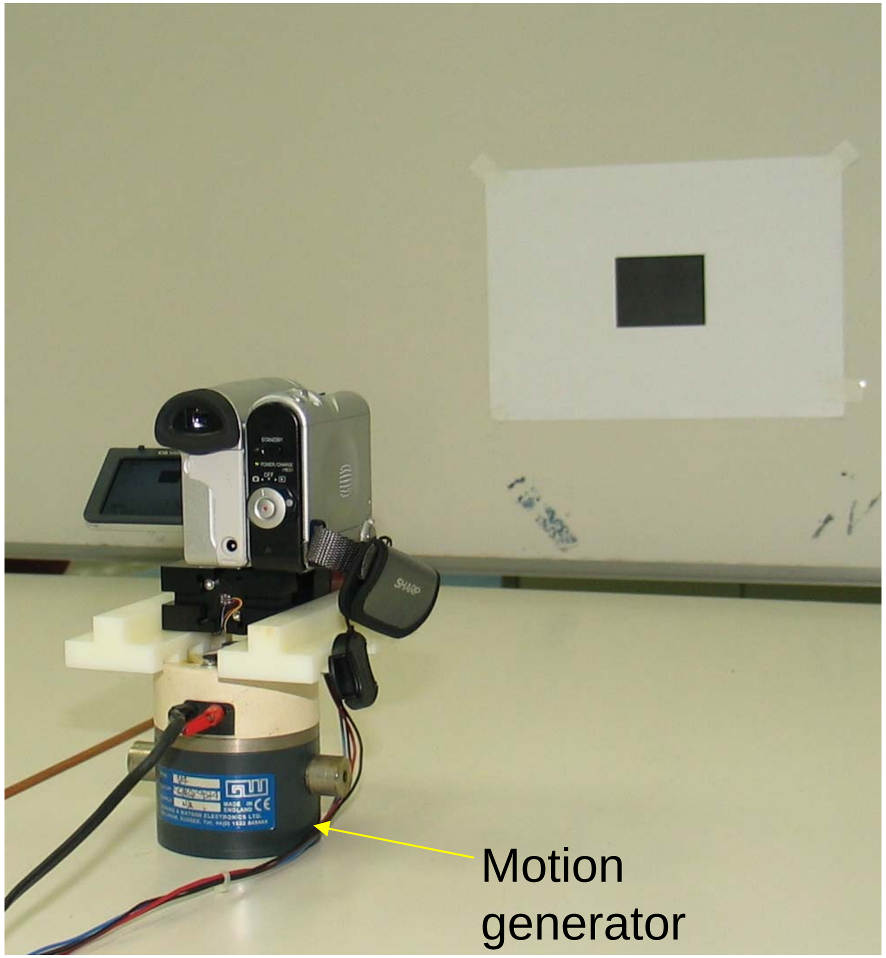

NANYANG TECHNOLOGICAL UNIVERSITY

Adaptive Phase Compensating Band-pass Filter

- Rmse:
  Raw footage
  = 2.61 pixels
  Compensated
  = 0.66 pixels
- Error reduction:
  75%

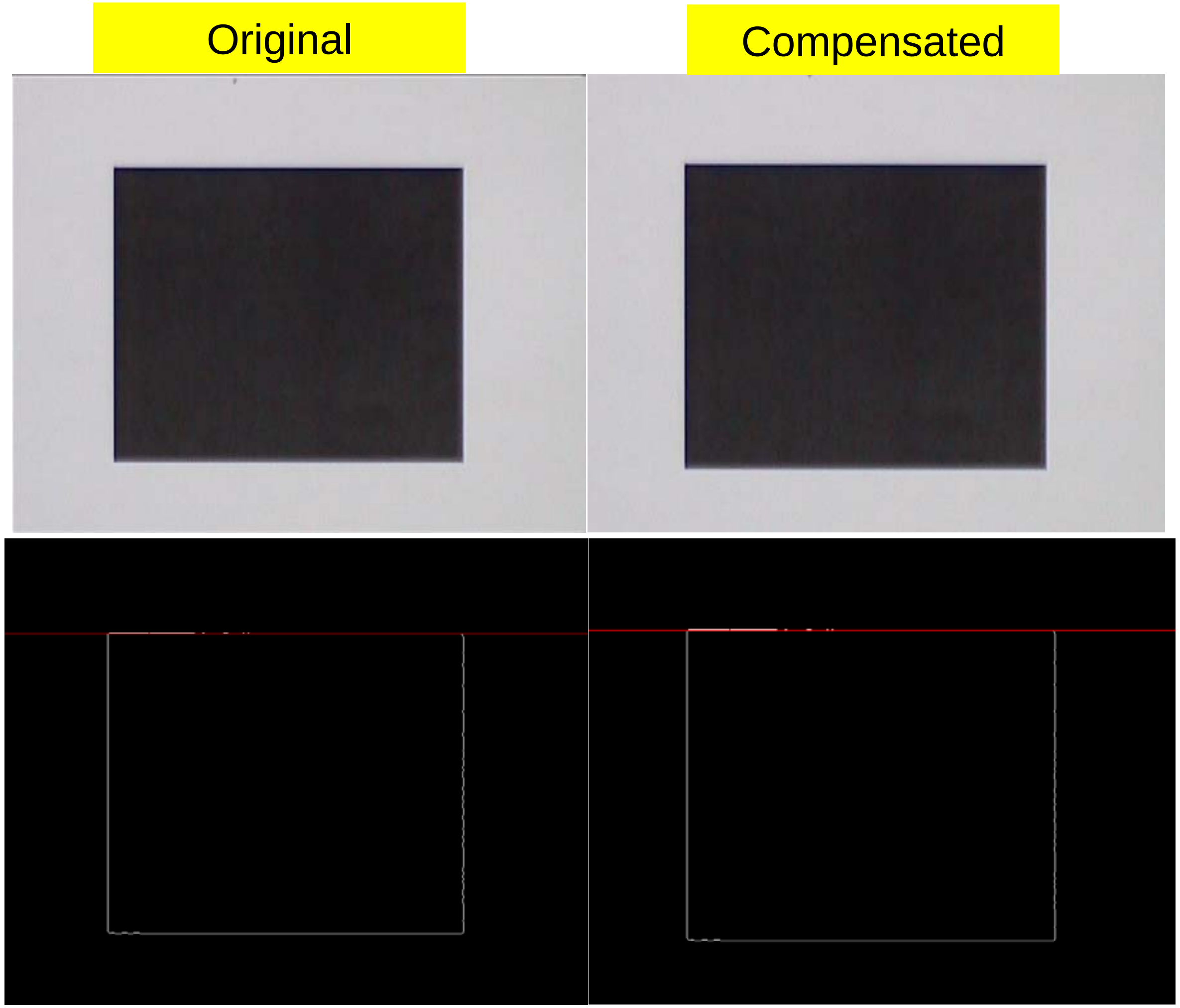

Microsurgery with Active Handheld Instrument

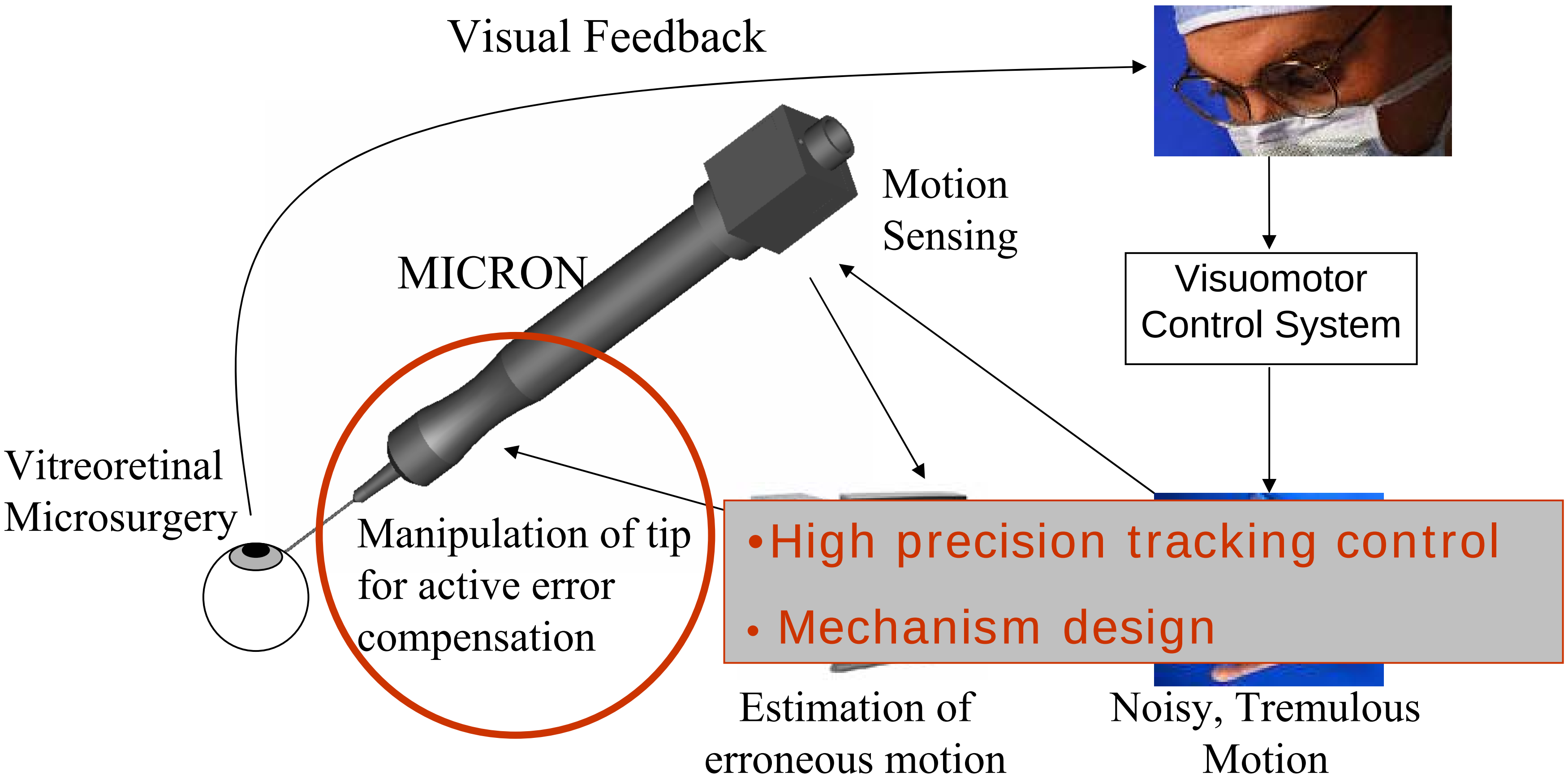

- High precision tracking control
- Mechanism design

Piezoelectric Actuator Hysteresis

- + :
  - High bandwidth
  - Fast response
  - High output force
- – :
  - Hysteresis
- ~15% of max. displacement

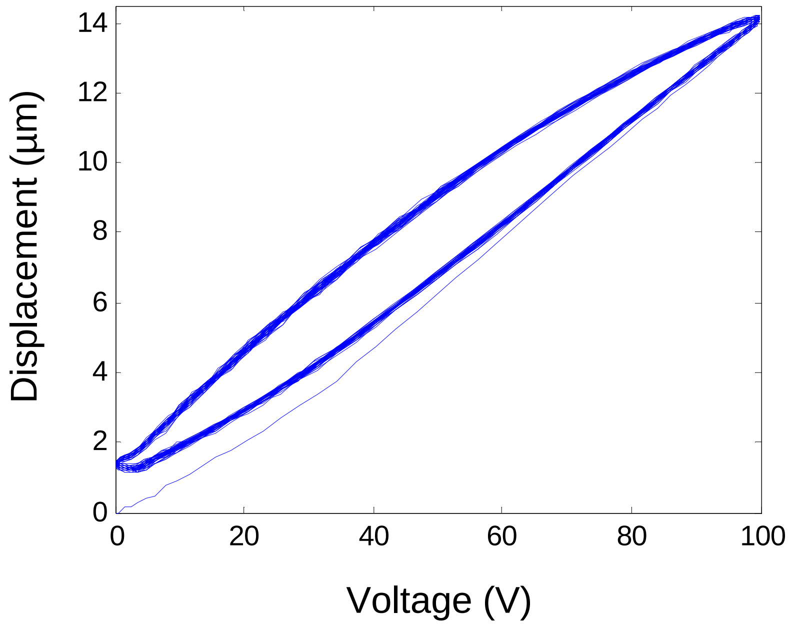

Commercial Piezo-System with Feedback Controller

- Piezo-driven 3 axis micro-positioner
  - Polytec-PI, Germany, NanoCube^{TM} P-611
  - >$ 10,000
  - Feedback sensors: strain gages
  - Tracking a 10 Hz, 100 μm p-p sinusiod
    - Hysteresis still present
    - Low-pass filtered behavior

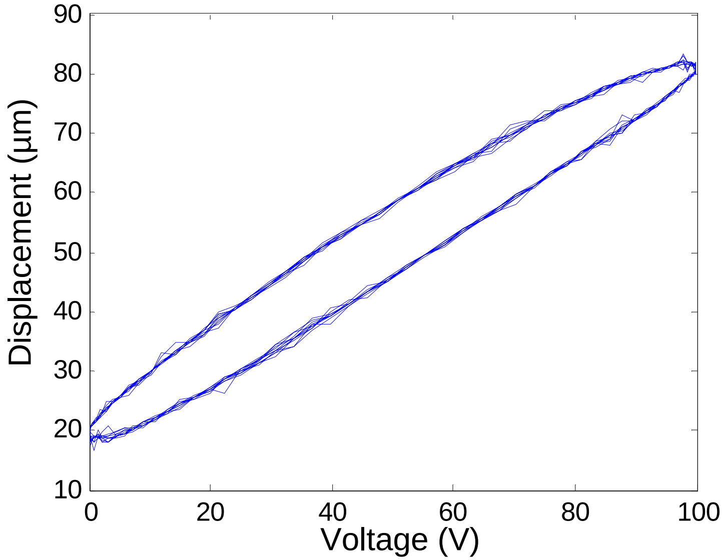

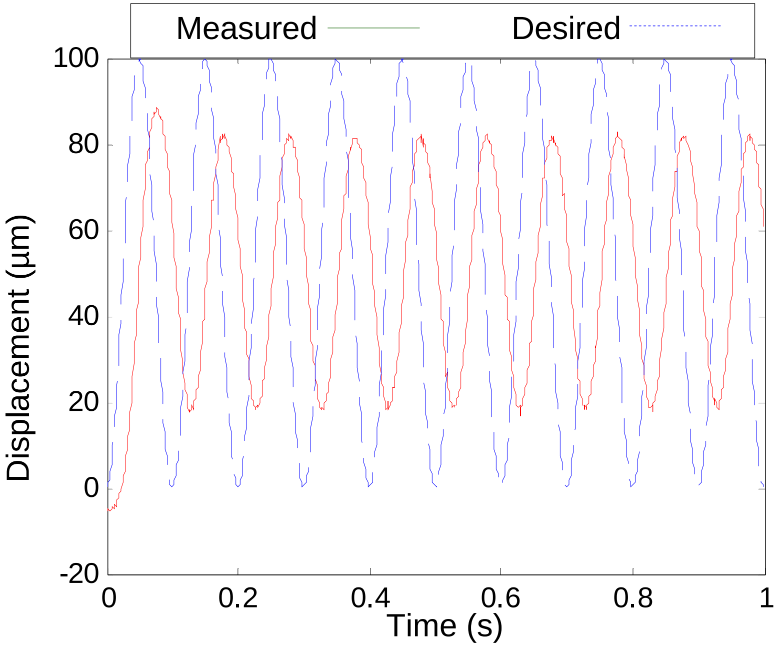

Open-loop Feedforward Controller with Inverse Hysteresis Model

- Develop a mathematical model that closely describes the hysteretic behavior of a piezoelectric actuator
- Existence of an inverse hysteresis model

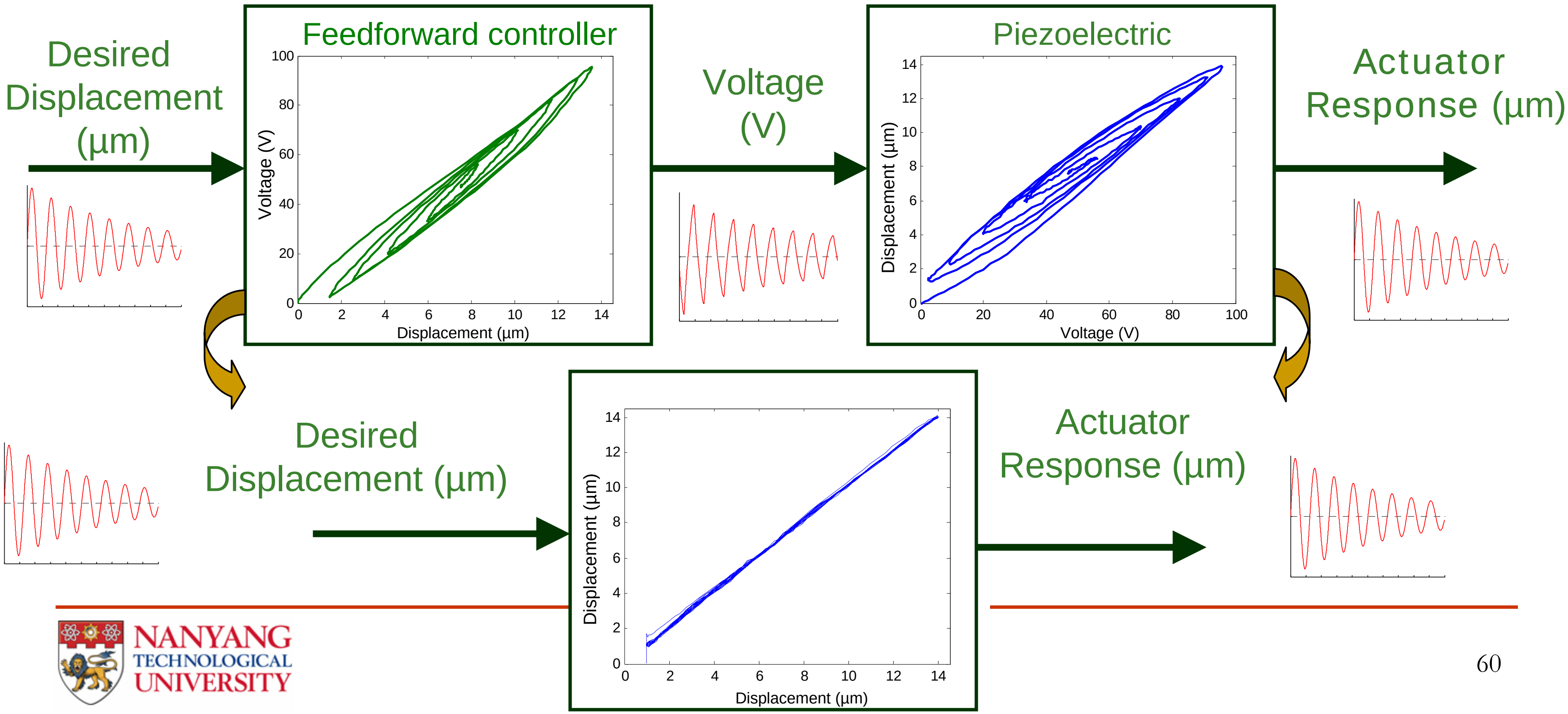

Prandtl-Ishlinskii (PI) Operator

- Rate independent backlash operator:

  $H_r = \max\{x(t) - r, \min\{x(t) + r, y_0\}\}$
- Linearly weighted superposition of backlash operators:

$$y(t) = \vec{w}_h^T \vec{H}_r [x, \vec{y}_0](t)$$

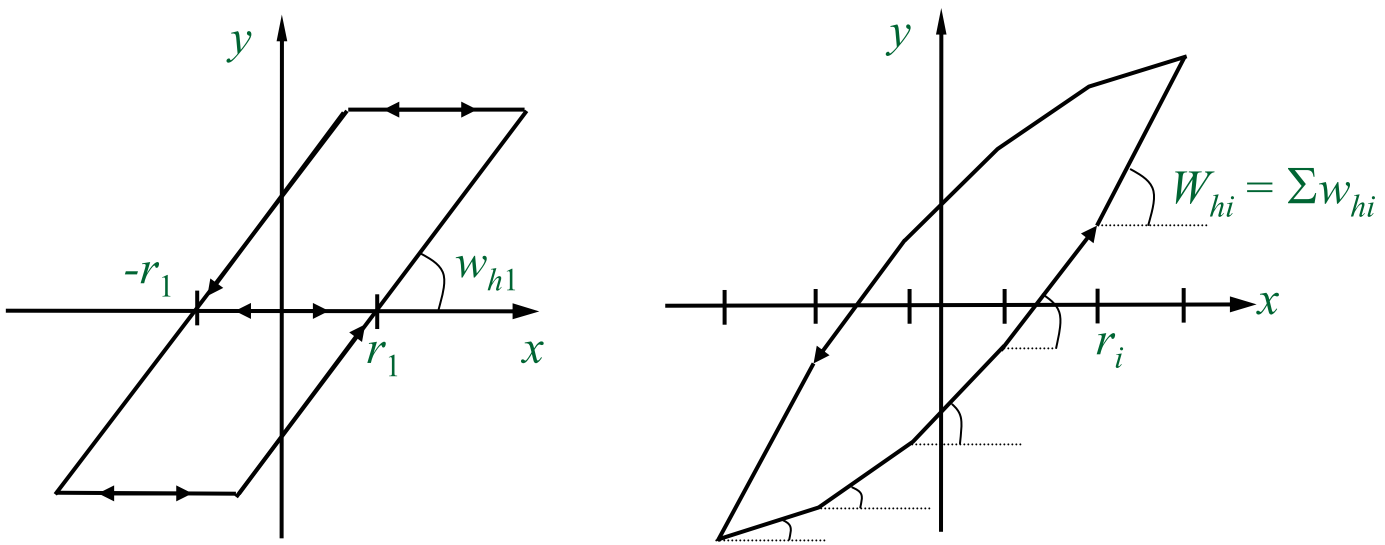

Modified PI Operator

- Backlash operators are symmetric but real hysteresis is not

PI model

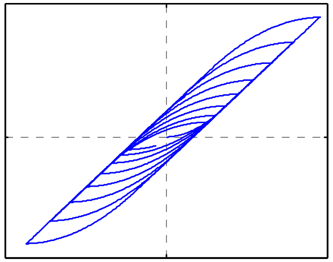

Real Hysteresis

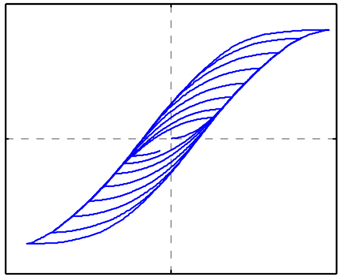

- Modeling saturation by linearly weighted superposition of dead-zone operators:

$$S_d[y](t) = \begin{cases} \max\{y(t) - d, 0\}, & d > 0 \\ y(t), & d = 0 \end{cases}$$

$$z(t) = \vec{w}_s^T \cdot \vec{S}_d[y](t)$$

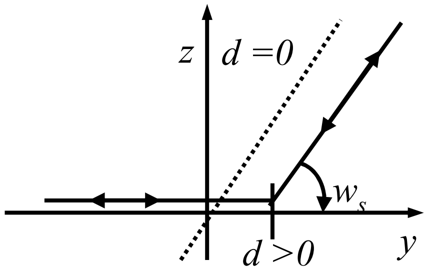

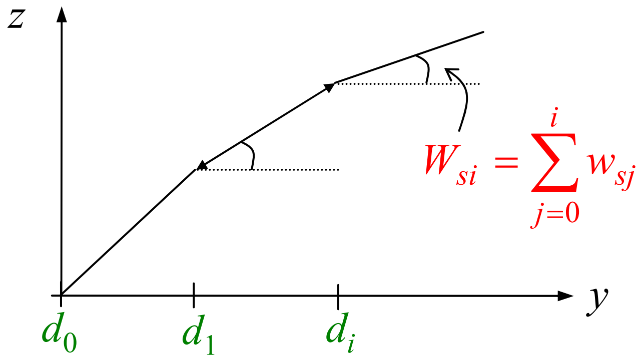

NANYANG TECHNOLOGICAL UNIVERSITY

Modified PI Operator

$$z(t) = \Gamma[x](t) = \vec{w}_s^T \cdot \vec{S}_d[\vec{w}_h^T \cdot \vec{H}_r[x, \vec{y}_0]](t)$$

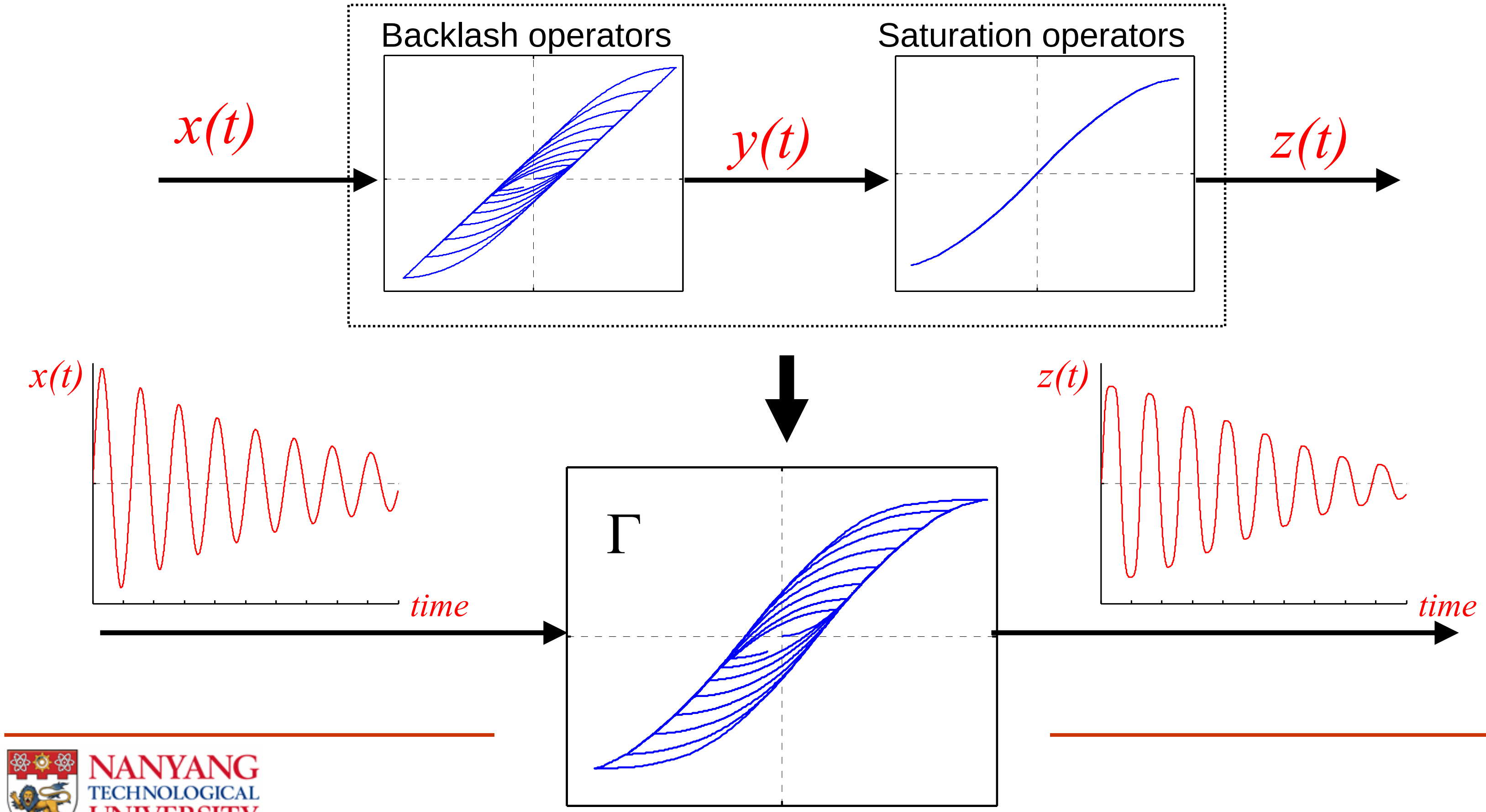

Inverse Modified PI Hysteresis Model

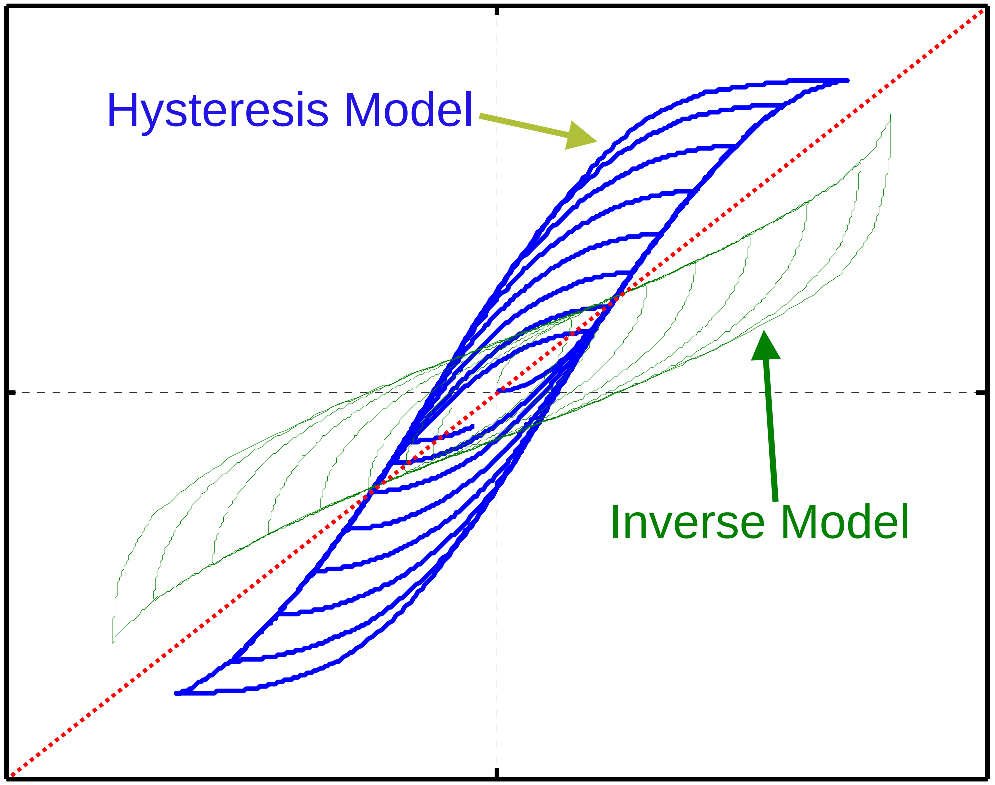

Inverse Modified PI Operator

$$\Gamma^{-1}[\hat{z}](t) = \vec{w}_h^{\prime T} \cdot \vec{H}_{r'}[\vec{w}_s^{\prime T} \cdot \vec{S}_{d'}[\hat{z}], \vec{y}'_0](t)$$

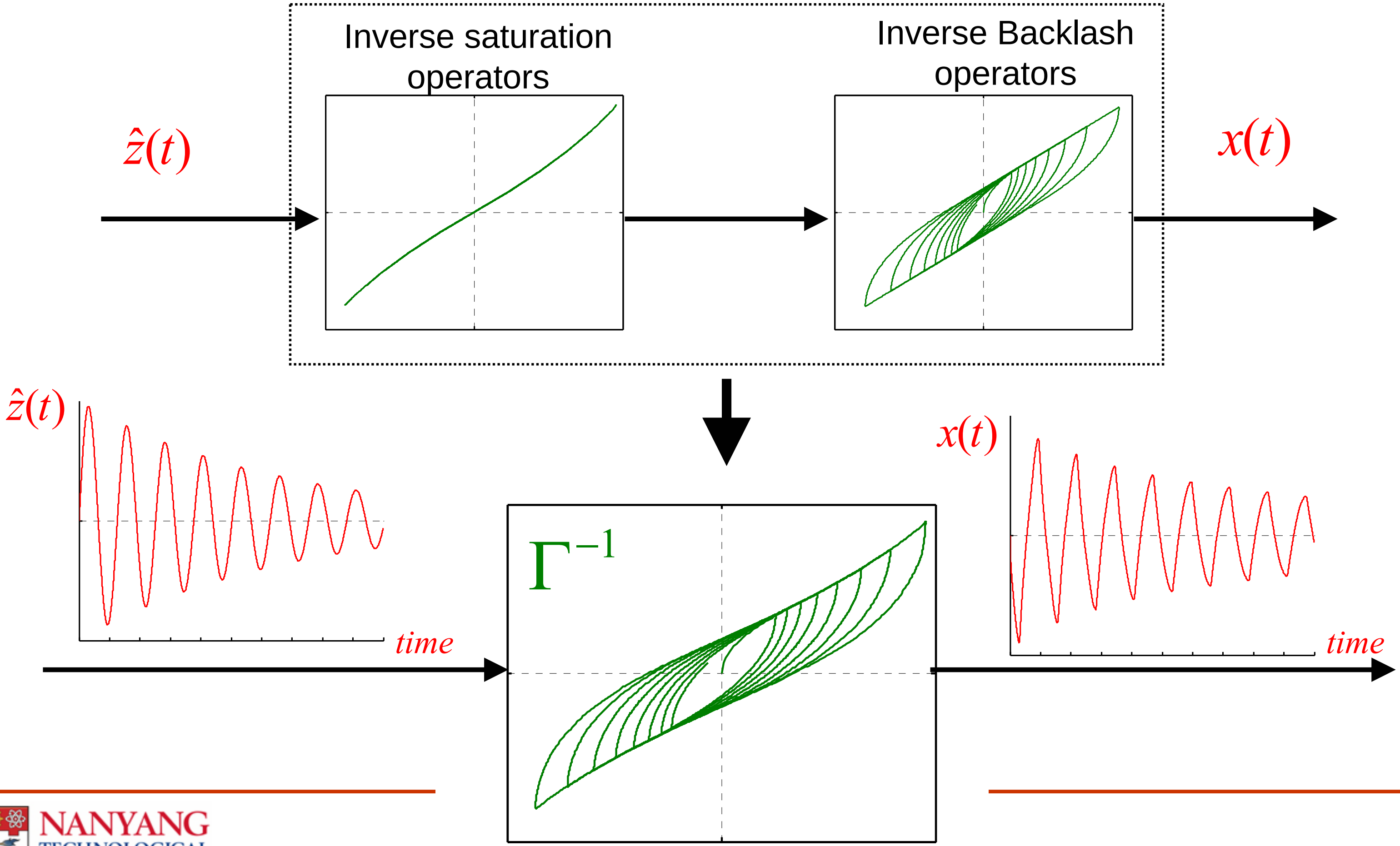

Piezoelectric Hysteresis is Rate Dependent

- Basic assumption of Prandtl-Ishlinskii operator:
  - Hysteresis is rate *in*dependent
- Our observation:
  - Hysteresis is rate *dependent*
- Tremor frequency is time varying and person specific
  - 8-12 Hz

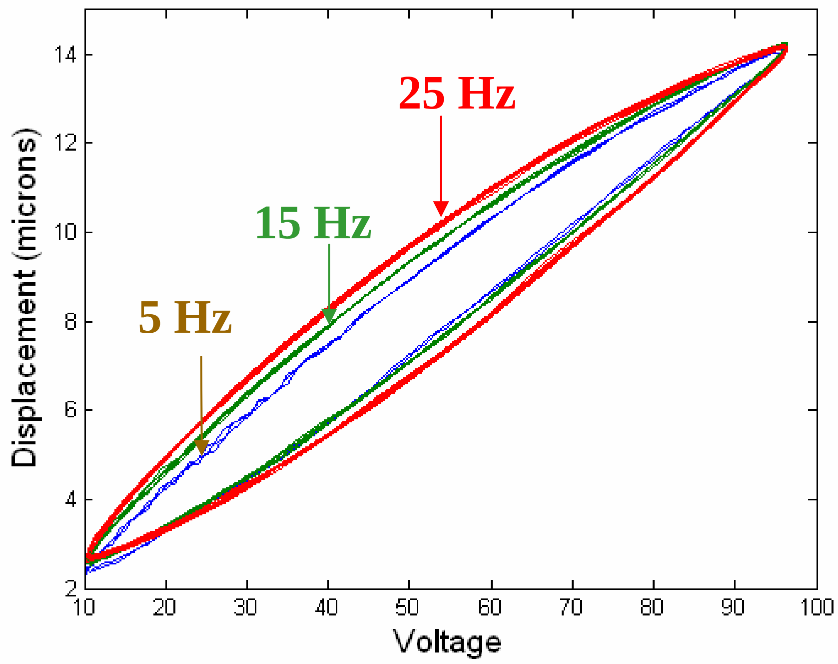

Rate-dependent PI Operator

- Assume saturation is rate independent
- Sum of the backlash weights up to r_i (slope of the hysteresis curve at interval i) is linearly dependent on actuation rate

$W_{hi} = \Sigma w_{hi};$

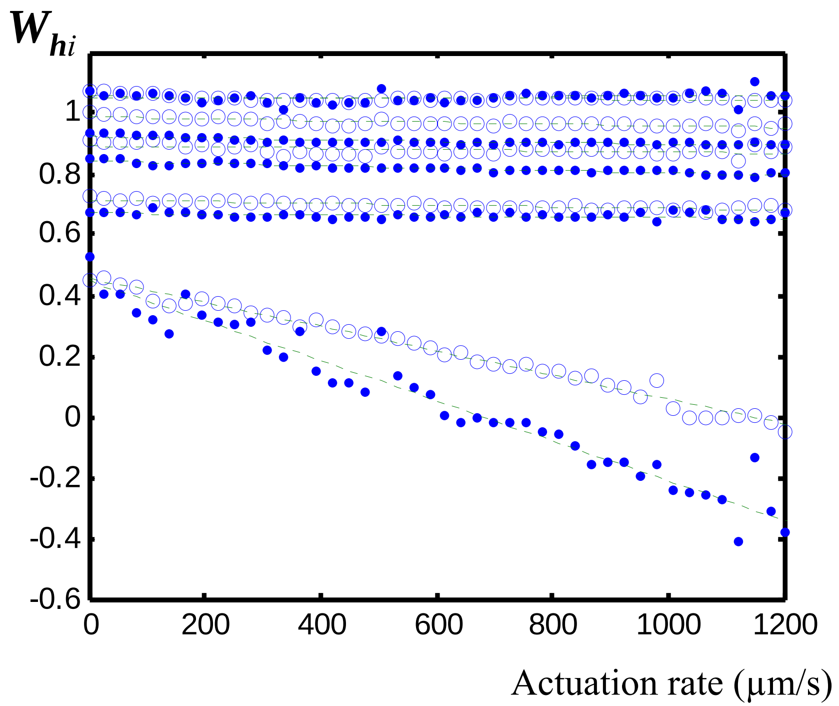

$$W_{hi}\left(\dot{x}(t)\right) = W_{hi}\left(\dot{x}_0\right) + c_i \dot{x}(t),\ i = 0 \ldots n$$

NANYANG TECHNOLOGICAL UNIVERSITY

Rate Dependent PI Hysteresis Model

- Rate dependent model:

$$z(t) = \Gamma[x, \dot{x}](t) = \vec{w}_s{}^T \cdot \vec{S}_d[\vec{w}_h(\dot{x}(t))^T \cdot \vec{H}_r[x, \vec{y}_0]](t)$$

- Also a PI type $\rightarrow$ Inverse exists
- Rate dependent inverse model

$$\Gamma^{-1}[\hat{z}]\left(t\right) = \vec{w}'_h(\dot{x}(t))^T \cdot \vec{H}_{r'(\dot{x}(t))}[\vec{w}'^T_s \cdot \vec{S}_{d'}[\hat{z}], \vec{y}'_0](t)$$

NANYANG TECHNOLOGICAL UNIVERSITY

Open-Loop Feedforward Controller with Inverse Rate-Dependent PI Hysteresis Model

- Tracking single frequency stationary sinusoids

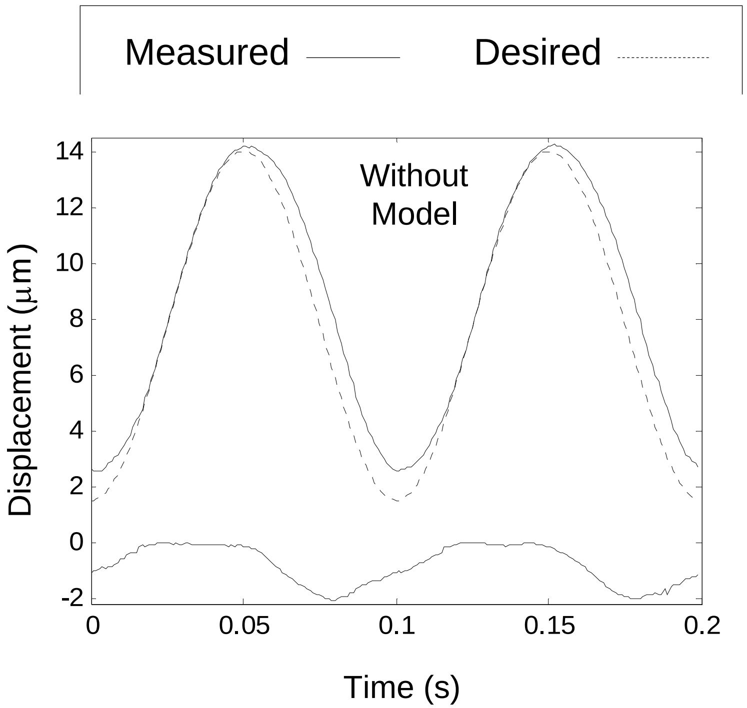

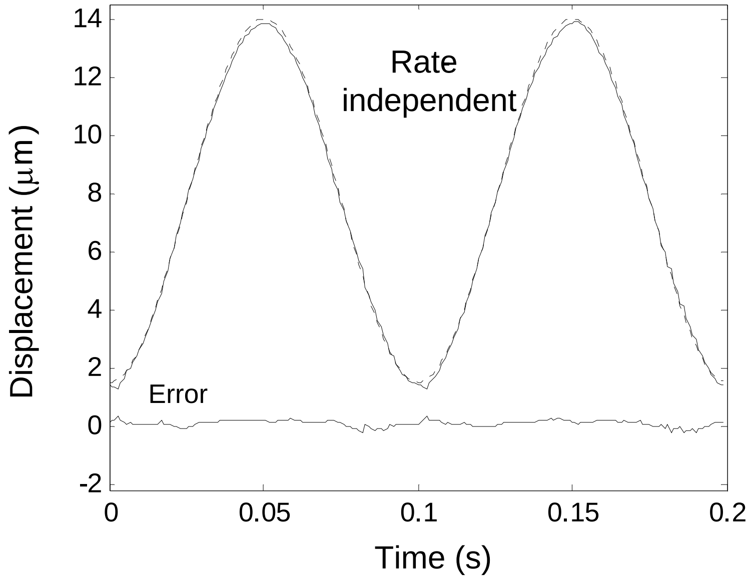

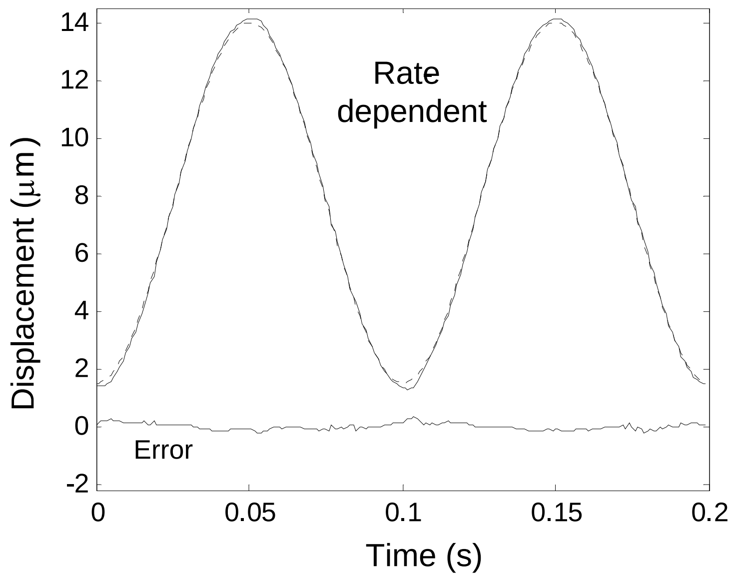

Open-Loop Feedforward Controller with Inverse Rate-Dependent PI Hysteresis Model

- Tracking multiple frequency non-stationary sinusoids

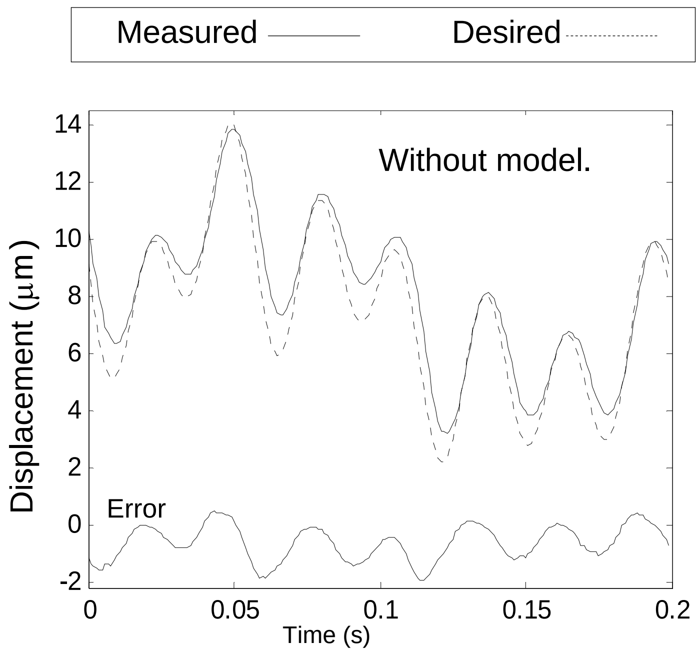

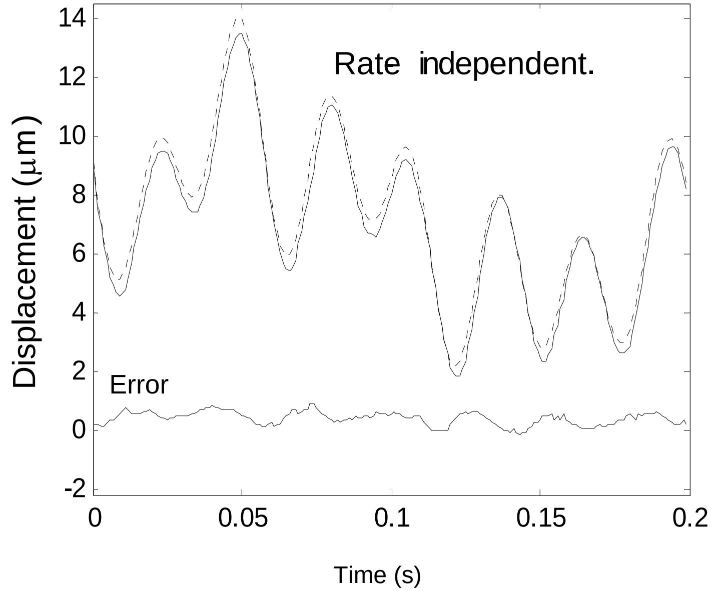

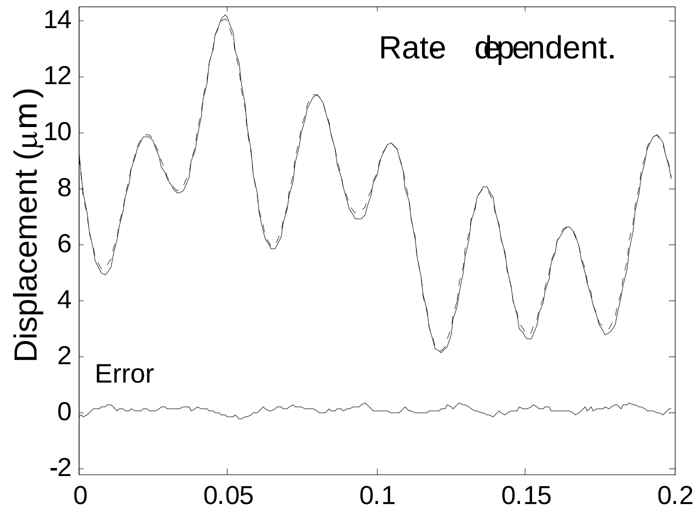

NANYANG TECHNOLOGICAL UNIVERSITY

Dynamic Motion Tracking Results

	Without model	Rate-independent	Rate-dependent
rmse $\pm\sigma$ (μm)	1.02 ± 0.07	0.31 ± 0.03	0.15 ± 0.003
$\frac{\text{rmse}}{\text{p - p amplitude}}(\%)$	9.2	2.8	**1.4**
max error $\pm\sigma$ (μm)	1.91 ± 0.08	0.89 ± 0.04	0.59 ± 0.06
$\frac{\text{max error}}{\text{p - p amplitude}}(\%)$	17.3	8.0	5.3

rms noise of interferometer = 0.01 μm

NANYANG TECHNOLOGICAL UNIVERSITY

Tremor Tracking Results

- Tracking recordings of real tremor using 1 piezoelectric stack
  - Rmse = 0.64% of max ampl.; Max error = 2.4% of max ampl.

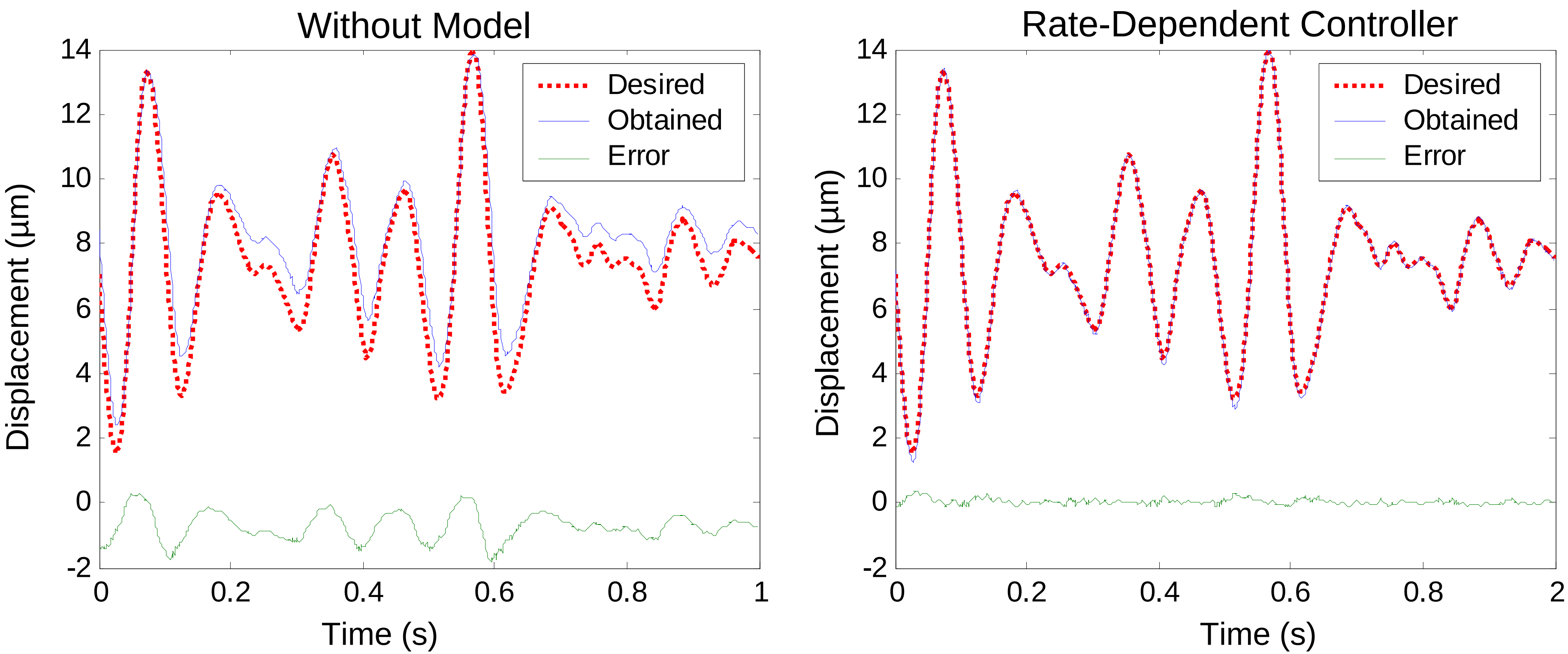

NANYANG TECHNOLOGICAL UNIVERSITY

Microsurgery with Active Handheld Instrument

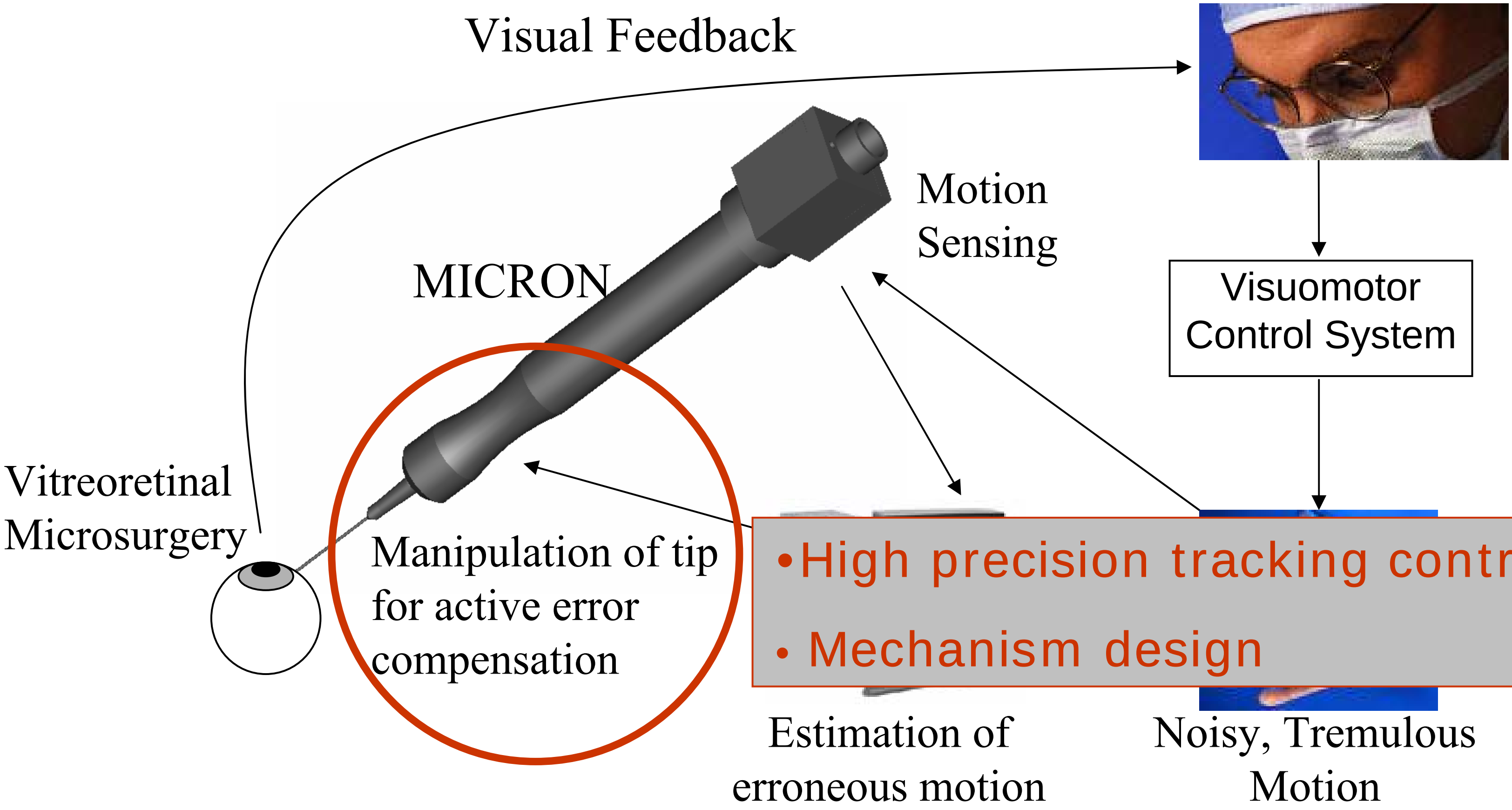

- High precision tracking control
- Mechanism design

Design of Parallel Mechanism

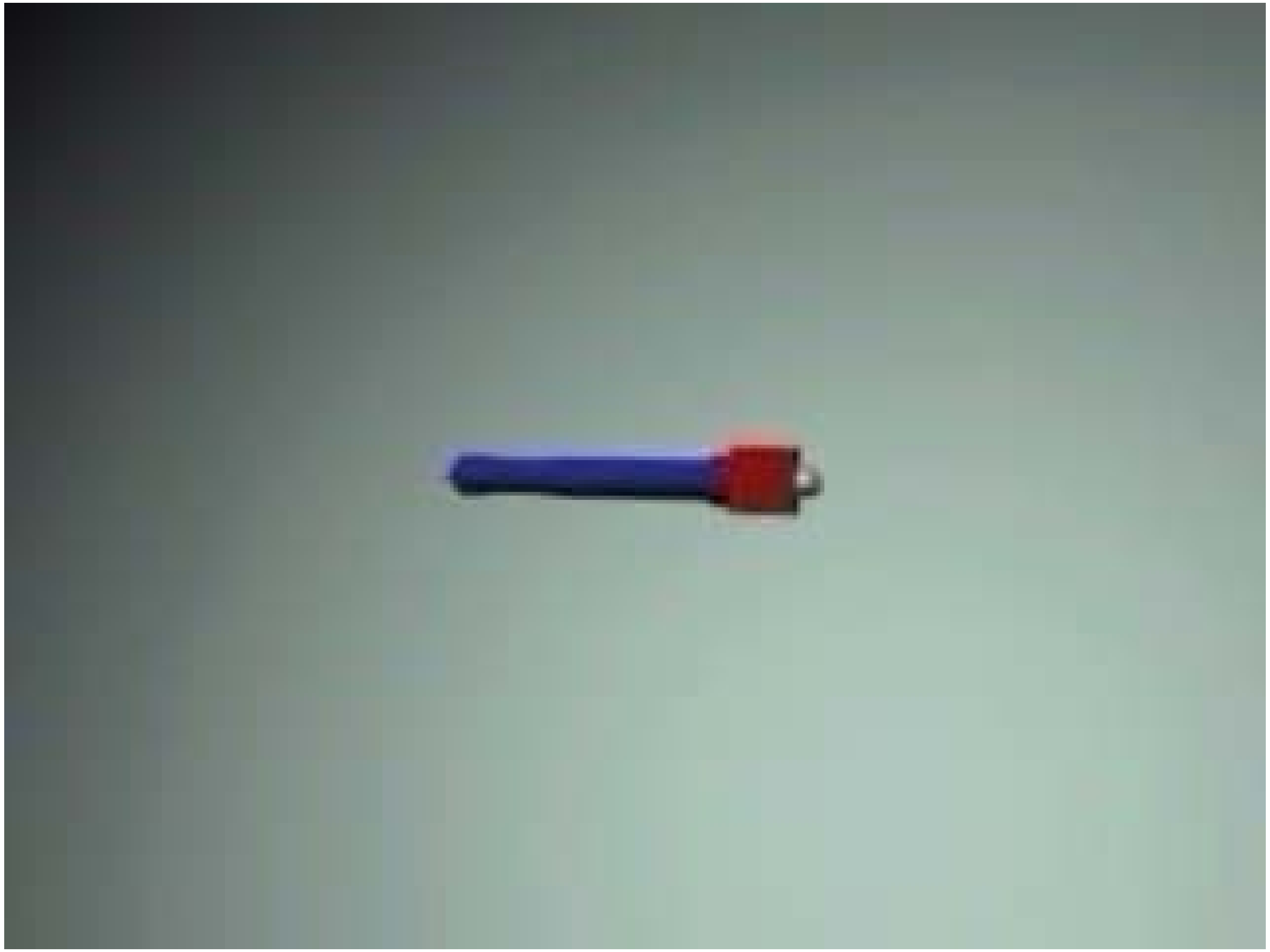

Manipulator Design

- 3 DOF piezoelectric-driven parallel manipulator
  - 1 actuator per axis, max effective stroke = 12.5 μm
  - Motion amplification = 9.4x, total stroke > 100 μm
- Tool tip approximated as a point, hence only 3 DOF manipulation
- Parallel manipulator design because
  - Rigidity, compactness, and design simplicity
- Located at the front end to balance the weight of the instrument

Design of Parallel Mechanism - New

- IEEE EMBS 2005 (Shanghai) Best Student Design Competition winner
  - David Choi et al.
- Monolith design using Stereolithography
- ∅22 x 58 mm

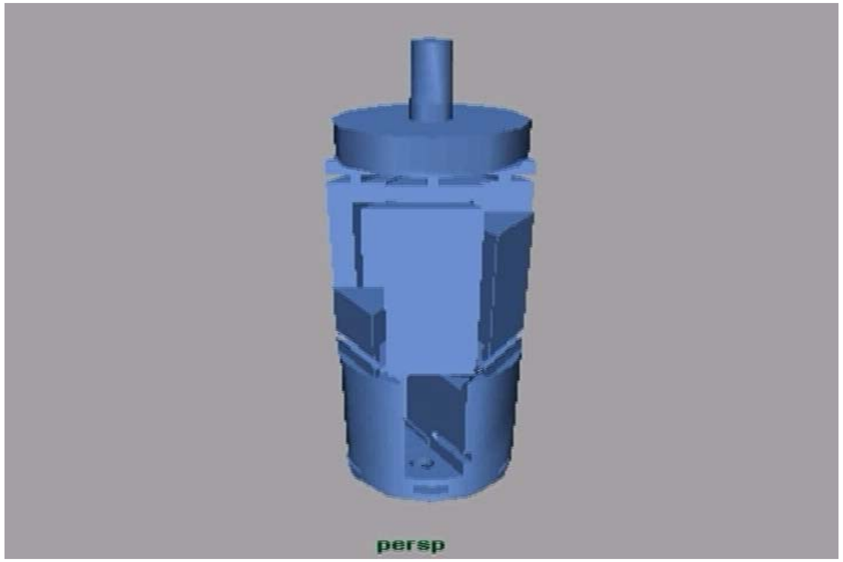

Manipulator Kinematics

- Inverse kinematics
  - Modeled as Lee & Shah RS-type
  - Closed-form solution
- No internal singularity

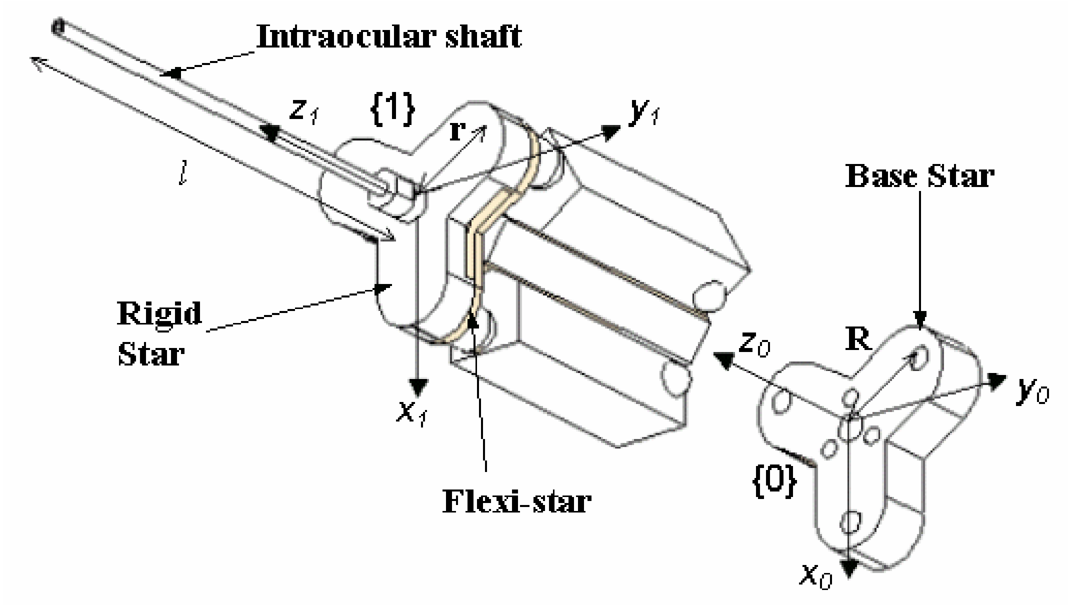

Workspace Analysis

- X_{max}, Y_{max} = 650 μm
- Z_{max} = 100 μm
- Tremor Space = ∅ 50 μm

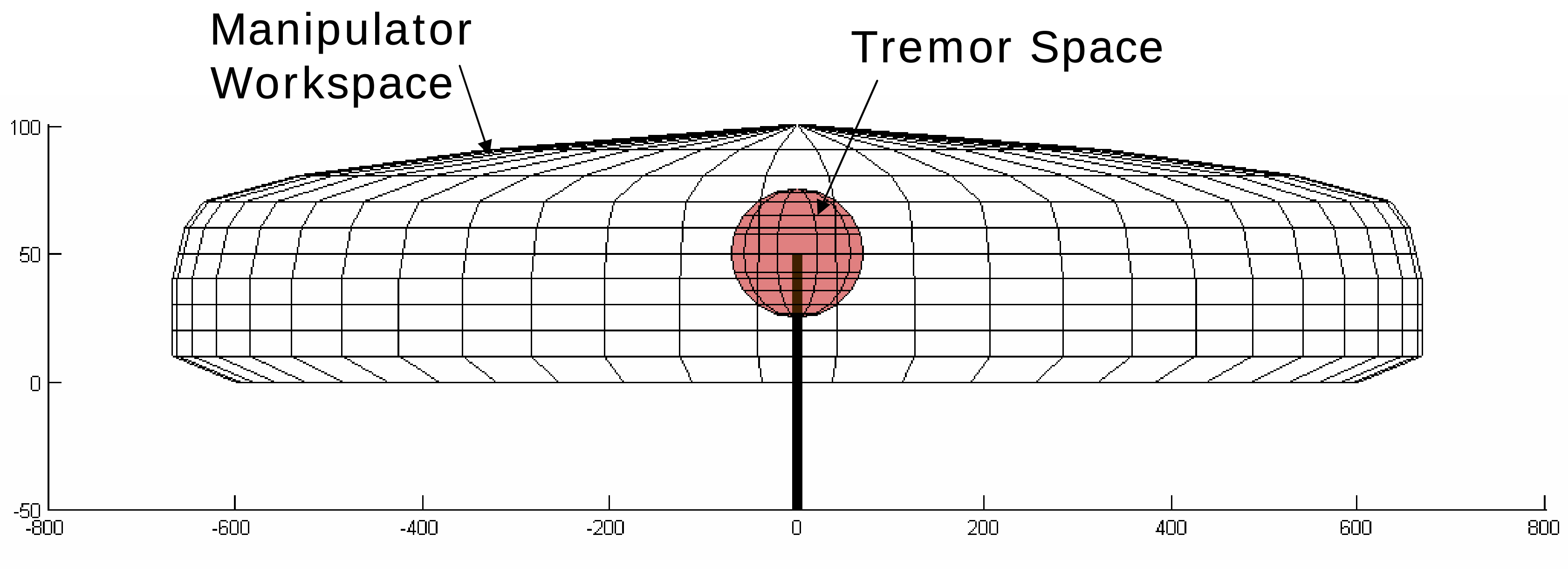

Manipulator 3D Tracking Result

- Tracking planar circle of ∅200 μm
- Mean tracking rmse ~ 12.1 μm

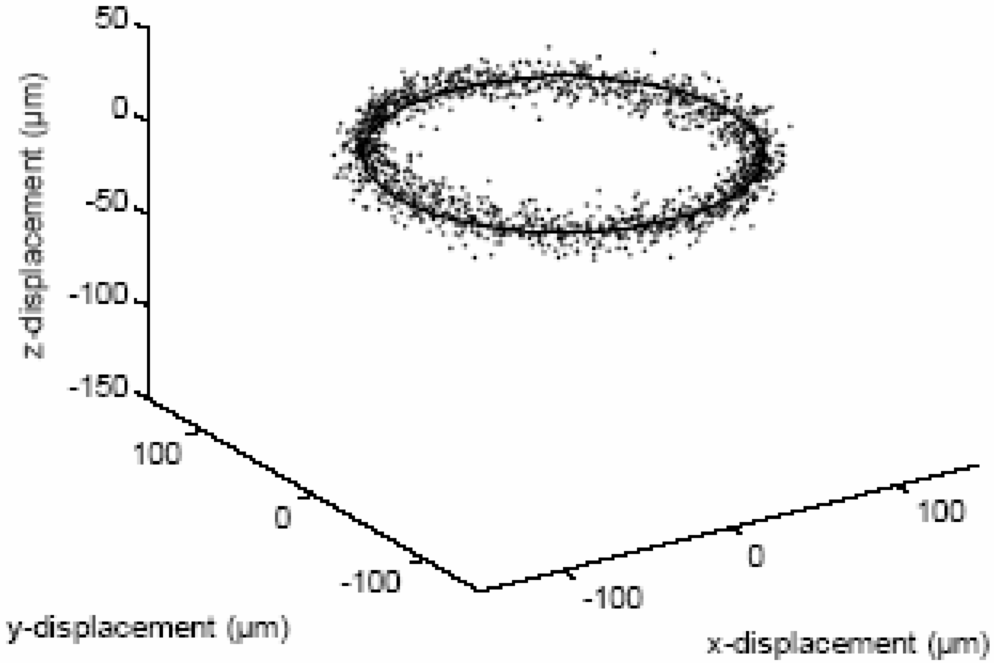

NANYANG TECHNOLOGICAL UNIVERSITY

Microsurgery with Active Handheld Instrument

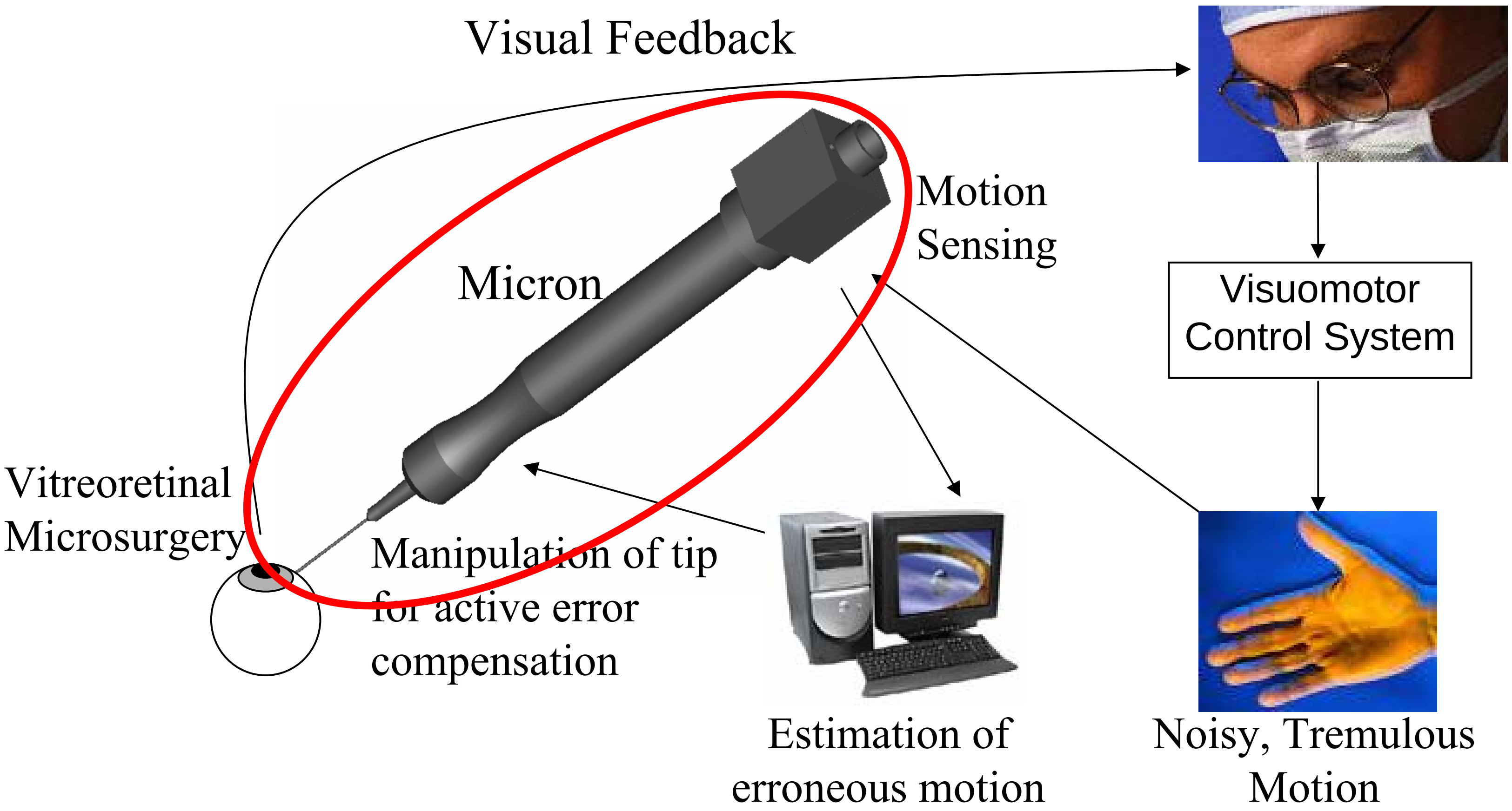

Motion Canceling Experiment

- Translation only
  - Generated motion: 9 Hz, 91 μm p-p
- Ave compensated tip motion over 10 runs = 60 μm p-p
- 34.3% reduction
- 3D optical sensing system
  - < 1.0 μm rms accuracy

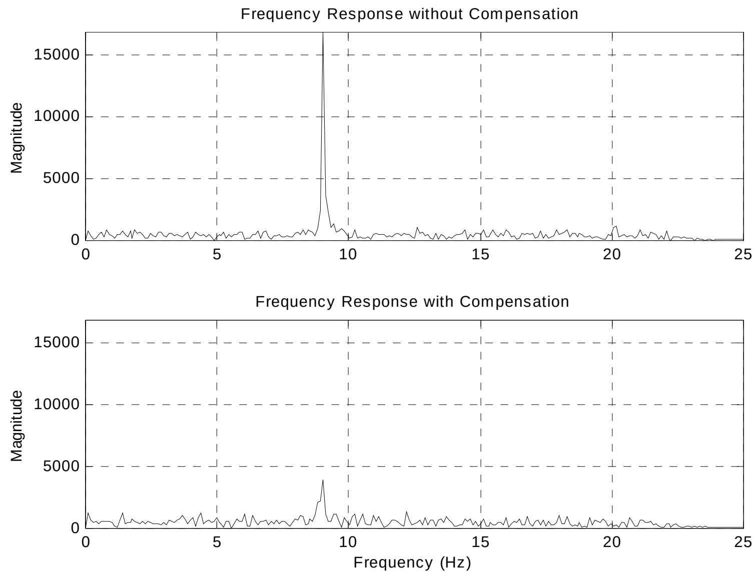

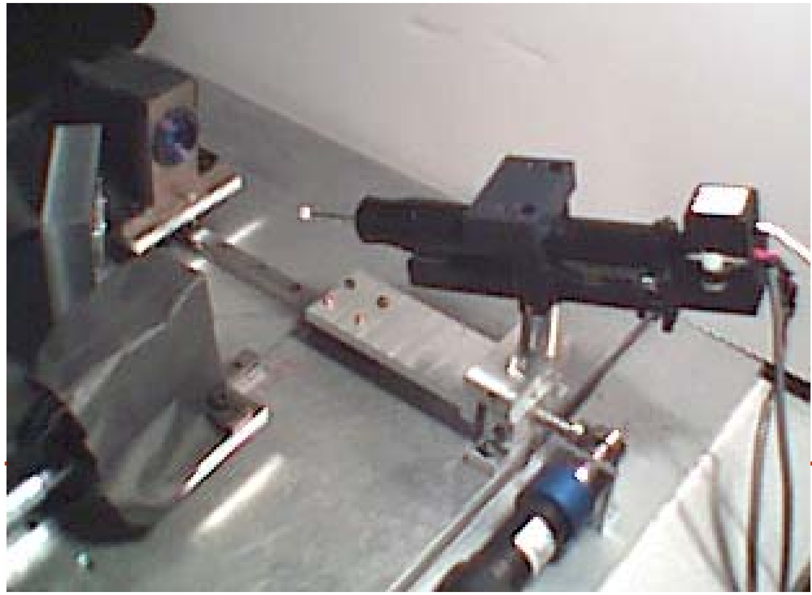

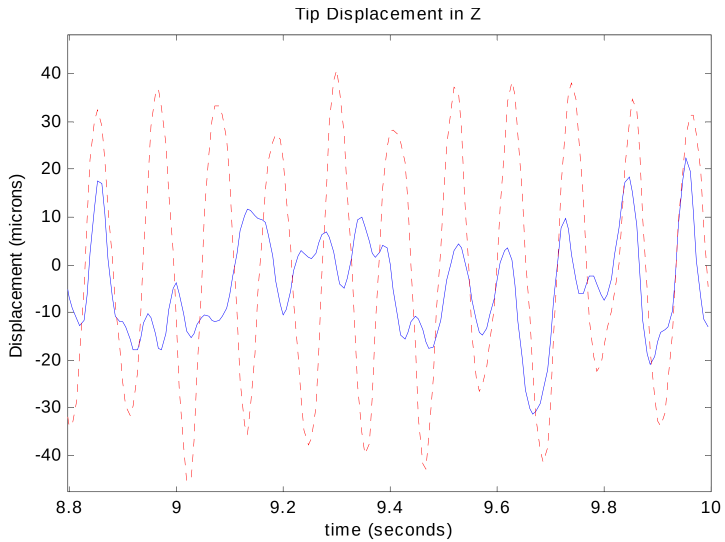

Motion Canceling Experiment

Micron Canceling Hand Tremor

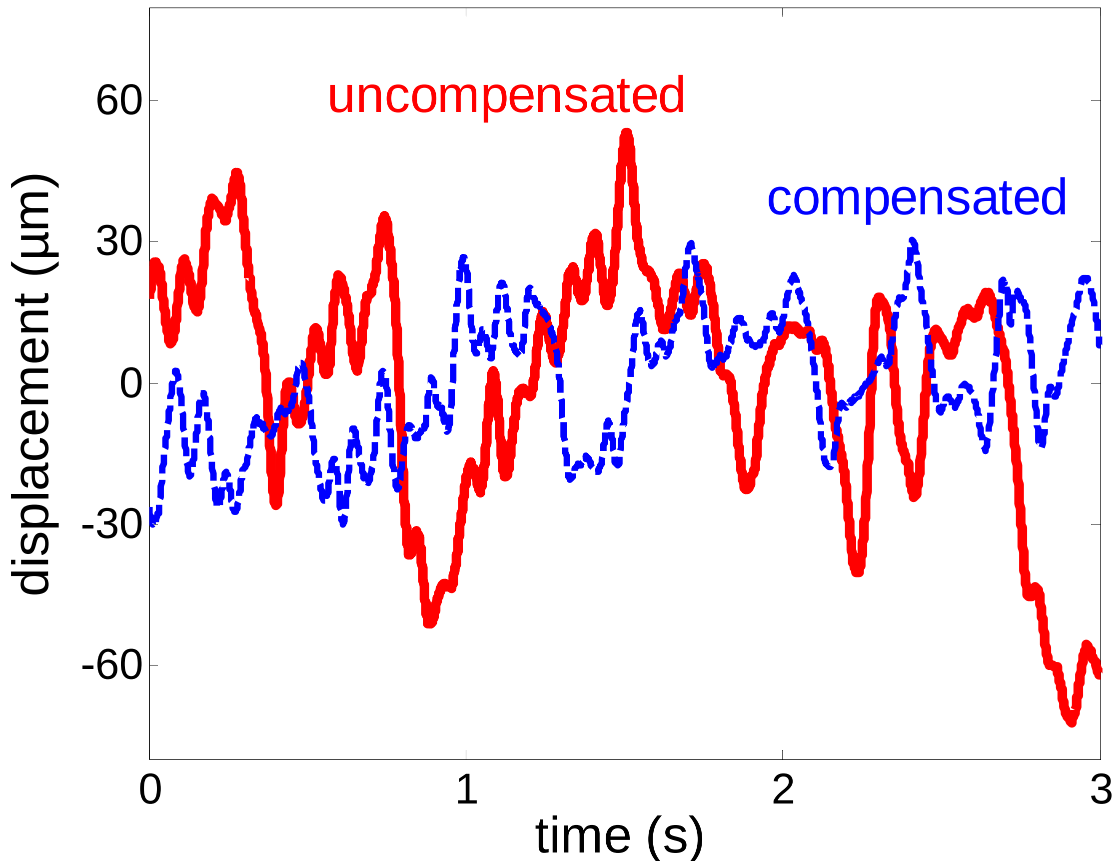

Total range:
52% reduction

RMS amplitude:
47% reduction

NANYANG TECHNOLOGICAL UNIVERSITY

Other Applications

- Surgery and Diagnostics

  Active compensation of periodic human physiological and pathological motion

  - Beating heart, breathing, etc.
  - Pathological tremor due to Parkinson's diseases, multiple sclerosis, etc.
- Military optical tracking devices
  - Handheld, vehicle & ship mounted
- Consumer camera/camcorder

Other Applications: Cell Manipulation / Dissection

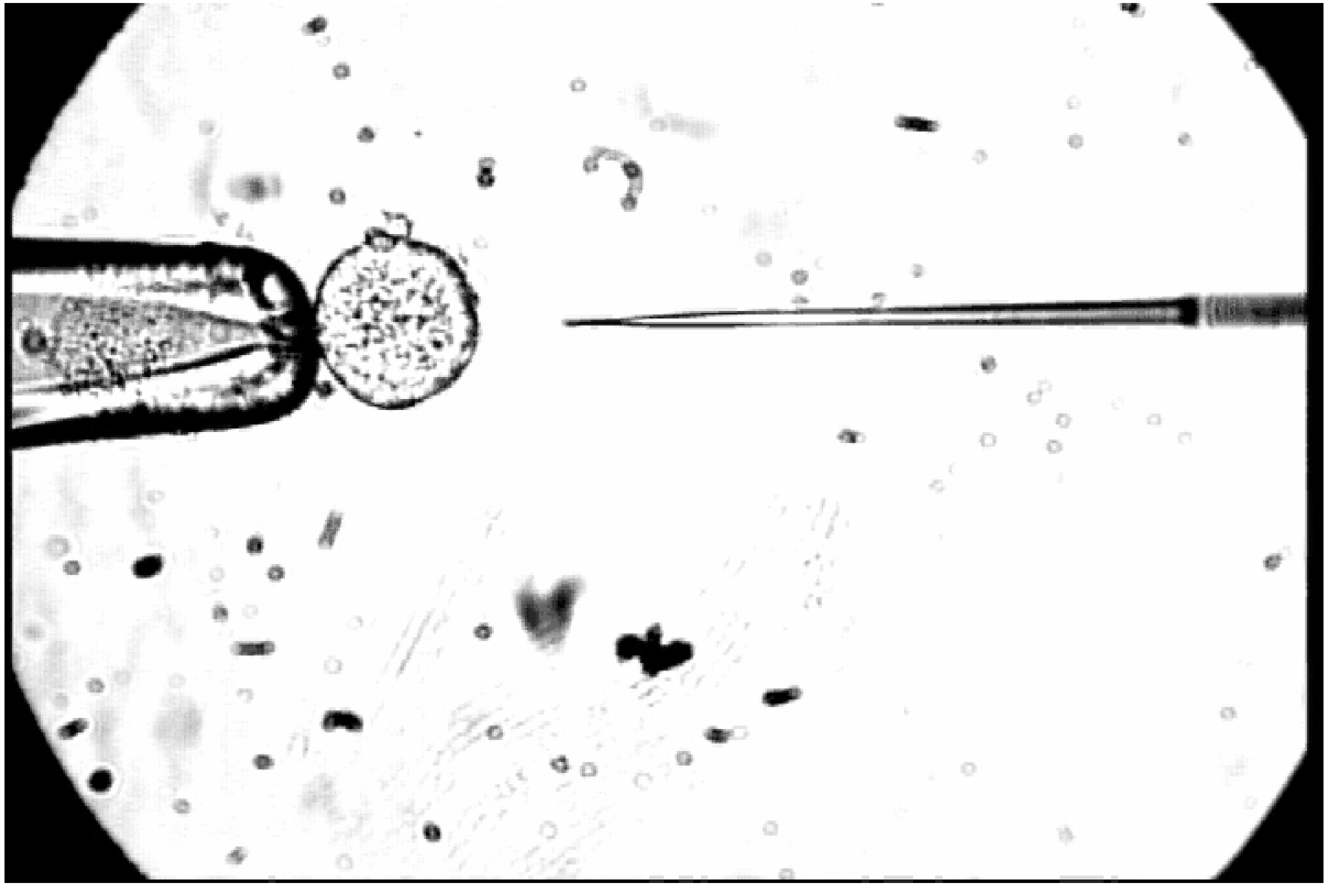

Questions & Comments

Wei Tech Ang

School of Mechanical & Aerospace Engineering

Nanyang Technological University

Singapore

wtang@ntu.edu.sg